Scilight

Innovations in Water Treatment
https://www.sciltp.com/journals/iwt



Review

Check for updates

Tailoring MOFs for Pollutant Removal and Catalysis: A Review on Defect Engineering, Doping, and Functionalization

Fan Yang [1], Jiaoping Wang [2], Xing Li [3], Han Li [1], Yan Feng [1,*], Yawen Yang [4,*]

[1] School of Civil Engineering and Architecture, University of Jinan, Jinan 250022, China
[2] Jinan Urban Construction Group Co., Ltd., Jinan 250022, China
[3] Environmental Engineering Co., Ltd., Shandong Academy of Environmental Science, Jinan 250001, China
[4] Institute of Urban Safety and Environmental Sciences, Beijing Academy of Science and Technology, Beijing 100054, China
* Correspondence: cea_fengy@126.com; Tel.: +86-13953135320

How To Cite: Yang, F.; Wang, J.; Li, X.; et al. Tailoring MOFs for Pollutant Removal and Catalysis: A Review on Defect Engineering, Doping, and Functionalization. *Innovations in Water Treatment* **2026**, *1*(1), 6. https://doi.org/10.53941/iwt.2026.100006

Received: 31 August 2026
Revised: 18 September 2026
Accepted: 21 September 2026
Published: 29 September 2026

Abstract: Metal–organic frameworks (MOFs) have attracted considerable attention in water treatment due to their high porosity, tunable pore structures, and large specific surface areas. This review summarizes advances from 2015 to 2025 in three modification strategies—defect engineering, metal-ion doping, and functionalization—and their applications in water pollutant adsorption, detection, and catalytic degradation. These strategies enhance performance by increasing active-site density, tuning electronic structures, and introducing specific host–guest interactions. Representative examples include defect-engineered MOFs for heavy-metal and phosphate adsorption, functionalized MOFs for sensitive contaminant sensing, and bimetallic MOFs for photocatalytic and persulfate-based advanced oxidation. The review also critically compares the three strategies and identifies key challenges in structural stability, scalable synthesis, and mechanistic understanding. Future research should prioritize the rational design of water-stable MOFs, machine-learning-assisted discovery, *in situ* characterization of defect–performance relationships, green scalable synthesis, and validation under realistic water matrices. This review provides a timely overview and outlines pathways toward practical MOF-based water treatment technologies.

Keywords: metal-organic frameworks (MOFs); modification strategies; defect engineering; functionalization; applications

1. Introduction

As a class of crystalline porous materials, MOFs have garnered significant attention in environmental engineering due to their exceptional physicochemical properties, including high porosity, precisely tunable pore architectures, and exceptionally large specific surface areas [1,2]. These distinctive features make MOFs highly attractive for diverse applications, including environmental remediation, energy storage, and catalysis [3,4]. In particular, recent studies have demonstrated their promise in water treatment, including the adsorptive removal of emerging contaminants [5], photocatalytic degradation of organic pollutants [6], and desalination [7]. The ability to tailor the structures and functionalities of MOFs through rational design and diverse modification strategies further enhances their versatility and potential across various fields.

Since their discovery in the mid-1990s, MOFs have attracted sustained research interest from the scientific community [8]. A pivotal advancement occurred in 1999 when Prof. Omar M. Yaghi's research group at the University of California, Berkeley, reported the synthesis of MOF-5 [9]. This breakthrough inaugurated a new era for MOFs, transitioning them from proof-of-concept materials to functional materials with demonstrated practical

Copyright: © 2026 by the authors. This is an open access article under the terms and conditions of the Creative Commons Attribution (CC BY) license (https://creativecommons.org/licenses/by/4.0/).
Publisher's Note: Scilight stays neutral with regard to jurisdictional claims in published maps and institutional affiliations.

utility. Despite extensive research, most existing reviews focus on a single modification strategy or a single application, and an integrated overview linking modification strategies to water-treatment performance is still lacking. This review covers the period from 2015 to 2025 and aims to fill this gap.

Although several reviews have surveyed MOFs for environmental applications, most are organized around a single modification strategy (e.g., defect engineering or metal-ion doping) or a single application (e.g., adsorption or photocatalysis). A critical integration of the three principal modification strategies—defect engineering, metal-ion doping, and functionalization—with the three core water-treatment functions—adsorption, detection, and catalytic degradation—is still lacking. This review fills that gap. Its unique contributions are threefold: (i) it systematically compares the three modification strategies in terms of activity, selectivity, stability, scalability, and limitations; (ii) it links each strategy to specific water-treatment outcomes and mechanistic pathways; and (iii) it identifies design principles and future priorities for translating MOFs from laboratory studies to practical water treatment. To maintain a clear focus, this review deliberately excludes applications unrelated to water treatment, such as energy storage, supercapacitors, fuel cells, and drug delivery, except where they provide fundamental insight into modification–property relationships. By concentrating on water treatment, we aim to provide an application-oriented and critical guide for designing MOFs for real-world water purification, sensing, and catalytic remediation.

To better position MOFs among advanced materials for water treatment, it is instructive to compare them with several other prominent classes of porous materials. Covalent organic frameworks (COFs) are constructed via covalent bonds, which often endow them with superior chemical and thermal stability compared with many MOFs; however, their crystalline order and pore-size tunability are generally more limited, and their functionalization chemistry is less developed [10]. Metal oxides (e.g., TiO_2, ZnO, Fe_3O_4) exhibit excellent stability and low cost, and some possess intrinsic photocatalytic or magnetic properties, but they typically suffer from relatively low specific surface areas and a limited number of accessible active sites [11–13]. Carbon-based materials (e.g., activated carbon, graphene, carbon nanotubes) offer high electrical conductivity, good chemical stability, and scalable production, yet their pore structures are less precisely controllable, and their surface chemistry is less diverse than that of MOFs [14]. In contrast, MOFs distinguish themselves through exceptionally high surface areas, atomically precise pore architectures, and unparalleled tunability of metal nodes and organic linkers, which together enable rational design of host–guest interactions [1,15]. Nevertheless, MOFs are often hampered by limited water stability, metal-ion leaching, and challenges in scalable synthesis—issues that are less pronounced for metal oxides and carbon materials [16,17]. These trade-offs suggest that the most promising path forward may not be the replacement of one material class by another, but rather the rational integration of MOFs with stable supports, protective coatings, or complementary materials to harness their respective strengths while mitigating their weaknesses. These considerations further justify the focus of this review on defect engineering, metal-ion doping, and functionalization for water treatment applications.

Key modification strategies, including defect engineering, metal ion doping, and functional group introduction, have been explored to enhance the performance of MOFs [2,18]. These modifications have significantly improved their catalytic activity, adsorption capacity, and stability, making them more suitable for practical applications. In particular, the application of MOFs in areas such as gas adsorption, water purification, and energy storage has demonstrated tremendous promise. Furthermore, this review will also discuss the challenges and limitations associated with the current state of MOFs. These include their long-term stability under operational conditions [2,3], the scalability of synthesis methods [19,20], and the need for a deeper understanding of reaction mechanisms [21]. By identifying these challenges, future research directions can be proposed to fully unlock the potential of MOFs in environmental engineering.

A systematic literature search was conducted using Web of Science, Scopus, PubMed, and Google Scholar. The search covered the period from 2015 to 2025. The following keyword combinations were used: (“metal–organic framework” OR “MOF” OR “MOFs”) AND (“defect engineering” OR “metal doping” OR “metal-ion doping” OR “functionalization” OR “ligand modification” OR “bimetallic MOF”) AND (“water treatment” OR “adsorption” OR “photocatalysis” OR “persulfate activation” OR “ozone catalysis” OR “sensing” OR “pollutant detection”). Only peer-reviewed journal articles, reviews, and high-quality conference proceedings published in English were considered. Studies were included if they (i) reported experimental data on MOF synthesis, modification, or application in water treatment, (ii) provided mechanistic insight into structure–property–performance relationships, or (iii) introduced novel modification strategies with clear relevance to environmental remediation. Studies were excluded if they (i) focused solely on applications unrelated to water treatment (e.g., energy storage, drug delivery) without offering transferable mechanistic insight, (ii) lacked sufficient experimental detail or characterization data, or (iii) were not available in full text. The initial search yielded approximately 1,200 records. After removing duplicates and screening titles and abstracts, 480 articles were selected for full-text assessment. Of these, 312 articles met the inclusion criteria and were included in this review. This systematic approach ensures that the review covers the most relevant and recent advances while maintaining a clear focus on water treatment applications.

In conclusion, this paper presents a timely and comprehensive review of MOFs, highlighting their modification strategies, applications, and prospects. It is anticipated that this review will serve as a valuable resource for researchers and practitioners in the field of environmental engineering, fostering further advancements in the development and utilization of MOF materials.

2. Representative MOF Families and Their Structural Features

MOFs can be classified according to different criteria, including the type of metal node, the nature of the organic linker, the underlying topology, or historical naming conventions. Because these criteria are not mutually exclusive, the families discussed below should be regarded as representative examples rather than a strict hierarchical classification. Among the most widely studied families are isoreticular metal–organic frameworks (IRMOFs) [22], zeolitic imidazolate frameworks (ZIFs) [23], porous coordination networks (PCNs) [24], and several other important families such as University of Oslo (UiO) [25], Materials of Institute Lavoisier (MIL) [26], and Hong Kong University of Science and Technology(HKUST-1) [27]. This section introduces the structural characteristics of these families and highlights their relevance to water treatment applications.

2.1. Isoreticular Metal-Organic Frameworks (IRMOFs)

The prototypical three-dimensional MOF, MOF-5, reported by Yaghi and co-workers in 1999 [9], served as the cornerstone of the IRMOF family. The term "isoreticular" refers to the retention of the same underlying topology while varying the length and functionalization of the organic linker. IRMOFs predominantly utilize zinc-oxo clusters as metal nodes [28], coordinated with dicarboxylate linkers such as 2,6-naphthalenedicarboxylic acid (2,6-H_2NDC) [29] and 4,4′-biphenyldicarboxylic acid(BPDC) [30,31]; N,N-Dimethylformamide(DMF) is commonly used as the solvent during framework assembly [32–35]. The combination of high structural symmetry and extended organic linkers endows IRMOFs with exceptionally large pore volumes, which primarily facilitates their applications in gas storage and separation systems, including hydrogen storage and carbon dioxide capture [36]. Although IRMOFs have also been explored for drug delivery [35], their inherent porosity renders them susceptible to structural degradation in aqueous environments. A notable advancement by Zhang et al. [32]demonstrated that immediate impregnation of IRMOF-3 with metal-based ionic liquids effectively mitigates framework cleavage, while encapsulation within polydimethylsiloxane (PDMS) membranes significantly enhances extraction performance. These efforts highlight both the potential and the stability challenges of IRMOFs in water-related applications.

2.2. Zeolitic Imidazolate Frameworks (ZIFS)

ZIFs are a specialized subclass of MOFs in which transition-metal ions (e.g., Zn^{2+}, Co^{2+} [37], Fe^{2+} [38], Cu^{2+} [39]) are coordinated by imidazolate or imidazole-derived linkers. The metal source is typically a transition metal ion [40], while the organic linker is imidazole or an imidazole derivative such as 2-methylimidazole (Hmim) [41] or benzimidazole (BIM) [42,43], analogous to the ligands of aluminosilicate zeolites [44]. The metal ion and the imidazolate ligand form a metal-imidazole-metal (M-Im-M) unit that resembles the Si–O–Si bond in traditional silica-based zeolites. This unique structure enables ZIFs to combine the high specific surface area and porosity of MOFs with the tunable characteristics and high stability of traditional zeolites [42]. Their topology resembles that of aluminosilicate zeolites, which contributes to their high thermal and chemical stability.

ZIFs can be divided into monometallic and bimetallic types. Compared with monometallic ZIFs, most bimetallic ZIFs-particularly Co-Zn ZIF [45], Co-Ni ZIF [46], Co-Fe ZIF [47], Co-Cu ZIF [48], and other Co-M (M=Mn, Mo, Ce, etc.) ZIFs [49–51] exhibit improved catalytic activity, as discussed later in this review. Because of their abundant reserves and outstanding performance, electrocatalysts based on first-row transition metals (Fe, Co, Ni) have received considerable interest. Cobalt-based components are regarded as promising candidates because of their abundance on Earth, high intrinsic catalytic activity, environmental friendliness, low cost, and simple chemistry for forming compounds in various valence states. Various cobalt-based compounds, such as cobalt oxides [52], cobalt phosphides [53], cobalt chalcogenides [37], cobalt based layer double hydroxides [23], and cobalt-based MOFs/ZIFs and their derivatives [54], have shown intrinsic activity towards the adsorption and catalytic degradation of pollutants, making Cobalt one of the most attractive element in this field.

2.3. Porous Coordination Networks (PCNs)

PCNs are a broad family of MOFs characterized by precisely tunable porosity and well-defined topologies. In this review, the abbreviation PCN refers to "porous coordination network", following its common usage in the MOF literature. The term "pocket-channel" is not used here as a classification name but describes a structural

feature—interconnected channels and cavities—that can be present in certain PCN materials. The primary difference from other classical metal-organic frameworks (MOFs) is that PCNs are designed by first targeting a specific topology and then selecting appropriate building blocks for synthesis, whereas classical MOFs are more often synthesized first, followed by structural characterization and topological analysis. PCNs explore rare or novel topologies—such as the augmented component series (acs) [55], square component unconnected net (scu) [56], four-connected two-nodal with a specific geometry (ftw) [57], and rare earth-hexacarboxylate topology (rht) [58]—and, through the strategic selection of metal ions, organic ligands, and control of synthesis conditions, enable systematic regulation of pore size parameters [59]. For example, pore sizes ranging from microporous to mesoporous and even macroporous can be obtained by varying the length and functional group of the ligand or adjusting the coordination geometry of the metal ion [24]. Certain MOFs also possess the structural feature of channel interconnection. An exemplar is JNU-2, constructed by a team from Jinan University comprising Zeng Heng, Lu Weigang, and Li Dan. This material exhibits a precisely controlled pore size at the channel-pore junction, and this interconnection has been demonstrated to enhance the mass-transfer efficiency, thereby improving performance in applications such as separations and catalysis [60].

It is well established that PCNs typically possess a high specific surface area, which provides a large number of active sites, thereby ensuring optimal performance in adsorption and catalysis. A significant quantity of gas molecules or reactants can be adsorbed on the surface of the pore channel, thus improving the efficiency and selectivity of the reaction. The structural versatility of PCNs-encompassing adjustable pore size, shape, chemical functionality, and framework composition-allows for rational design of materials tailored to specific requirements across diverse applications, including selective separation [60], catalytic transformations [59], and sensor technologies.

2.4. Other Representative MOF Families

In addition to IRMOFs, ZIFs, and PCNs, several other MOF families have shown considerable promise in water treatment, including UiO-type MOFs (Zr-based, e.g., UiO-66), MIL-type MOFs (e.g., MIL-100, MIL-101), and HKUST-1 (Cu-based). Beyond these specific families, a variety of construction strategies have been developed to tailor MOF structures and properties. These strategies leverage the symmetry and functionality of molecular building blocks in their reactions with metal ions to facilitate the formation of covalent solids with targeted open frameworks. Multidentate molecular components are employed to enhance thermal stability. In contrast, alternative strategies for MOFs involve the use of vacant electron orbitals from various transition metals complexed with long-chain organic linkers, as well as the functional groups present on multiple linkers, to achieve specific material properties [46,61]. These and other MOFs may forgo a high degree of symmetry and are instead designed to function differently through the use of various metals and the modification or replacement of organic linkers [54]. Such MOFs often sacrifice some adsorption capacity for pollutants and are instead designed for molecular recognition and sensing of water contaminants, which require higher precision [19,62]. These precision—demanding applications, such as molecular probing, will be further discussed in Section 4.2, highlighting how the tunable structures of MOFs meet such requirements.

3. Modification Strategies of MOFs

MOFs inherently exhibit a large specific surface area, high porosity, and tunable structures. To further tailor their properties and broaden their application scope, various modification strategies have been developed. Current efforts focus primarily on three approaches to optimize host–guest interactions: defect engineering, metal-ion doping, and functionalization. To avoid ambiguity, the key terms used in this review are defined below, and their relationships are summarized in Table 1.

3.1. Terminology and Classification of Modification Strategies

Defect engineering refers to the deliberate introduction and control of structural imperfections in a MOF lattice—such as metal-ion vacancies [63], linker vacancies [64], and topological defects—to tune its physicochemical properties. Metal-ion doping denotes the incorporation of foreign metal ions into the MOF framework, typically at metal nodes or clusters, to form bimetallic or multimetallic MOFs; it can be achieved during synthesis or post-synthetically. Ion exchange is a specific post-synthetic route in which existing metal ions or counterions in a MOF are replaced by other ions without altering the overall framework topology; when metal ions are exchanged, it serves as a sub-route of metal-ion doping. Linker modification refers to the covalent chemical modification of organic linkers—either before or after synthesis—without replacing the linker backbone, for example by introducing $–NH_2$, –COOH, or –OH groups. Functionalization is a broader term that encompasses linker modification as well as the grafting of functional groups onto metal nodes and the encapsulation of

functional species; its primary aim is to introduce specific chemical functionality for host–guest interactions [65,66]. Heterostructures are composite materials formed by combining MOFs with other functional materials (e.g., semiconductors, metal nanoparticles, carbon materials) to create interfaces or heterojunctions that enable synergistic effects; they are not a modification of the MOF itself but rather a combination strategy. MOF-derived materials are materials obtained by thermal or chemical transformation of MOFs (e.g., pyrolysis or calcination), such as porous carbons, metal oxides, and metal sulfides; in these materials, the original MOF framework is destroyed, and they are therefore not MOFs but derivatives.

In this review, the three core modification strategies are defect engineering, metal-ion doping (with ion exchange as a sub-route), and functionalization (with linker modification as a sub-route). Heterostructures and MOF-derived materials are treated as cross-cutting extensions and are discussed in the application sections where relevant, but they are not used as primary categories in the classification of modification strategies. These modification strategies are further illustrated in Figure 1.

Table 1. Definitions of key modification-related terms and their relationship to the core strategies in this review.

Term	Definition	Relationship to Core Strategies	Typical Methods
Defect engineering	Deliberate creation/control of structural imperfections (vacancies, topological defects) in the MOF lattice	Core strategy 1	Thermal treatment, modulator-assisted synthesis, ligand replacement, irradiation
Metal-ion doping	Incorporation of foreign metal ions into the MOF framework, forming bimetallic/multimetallic MOFs	Core strategy 2	One-pot synthesis, impregnation, post-synthetic exchange
Ion exchange	Post-synthetic replacement of existing metal ions or counterions with other ions without changing the framework topology	Sub-route of metal-ion doping	Solution-phase exchange, immersion in metal salt solutions
Linker modification	Covalent chemical modification of organic linkers without replacing the linker backbone	Sub-route of functionalization	Pre-synthetic ligand design, post-synthetic grafting
Functionalization	Introduction of functional groups onto linkers or metal nodes to create specific host–guest interactions	Core strategy 3 (includes linker modification)	Pre-synthetic functionalization, post-synthetic modification, grafting
Heterostructures	Composites of MOFs with other materials (semiconductors, metals, carbon) forming interfaces/heterojunctions	Cross-cutting extension	*In situ* growth, deposition, hybridization
MOF-derived materials	Materials obtained by thermal/chemical transformation of MOFs (e.g., porous carbons, metal oxides)	Cross-cutting extension	Pyrolysis, calcination, sulfidation

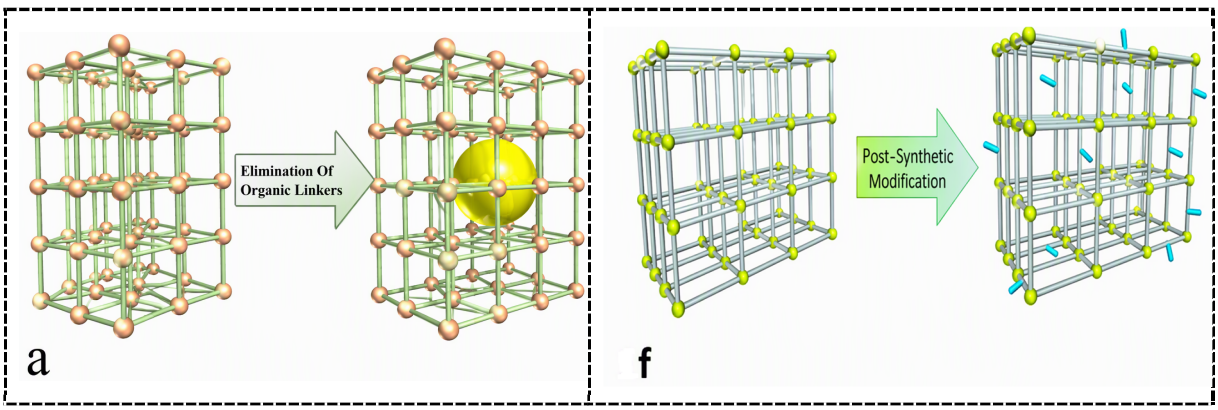


Figure 1. *Cont.*

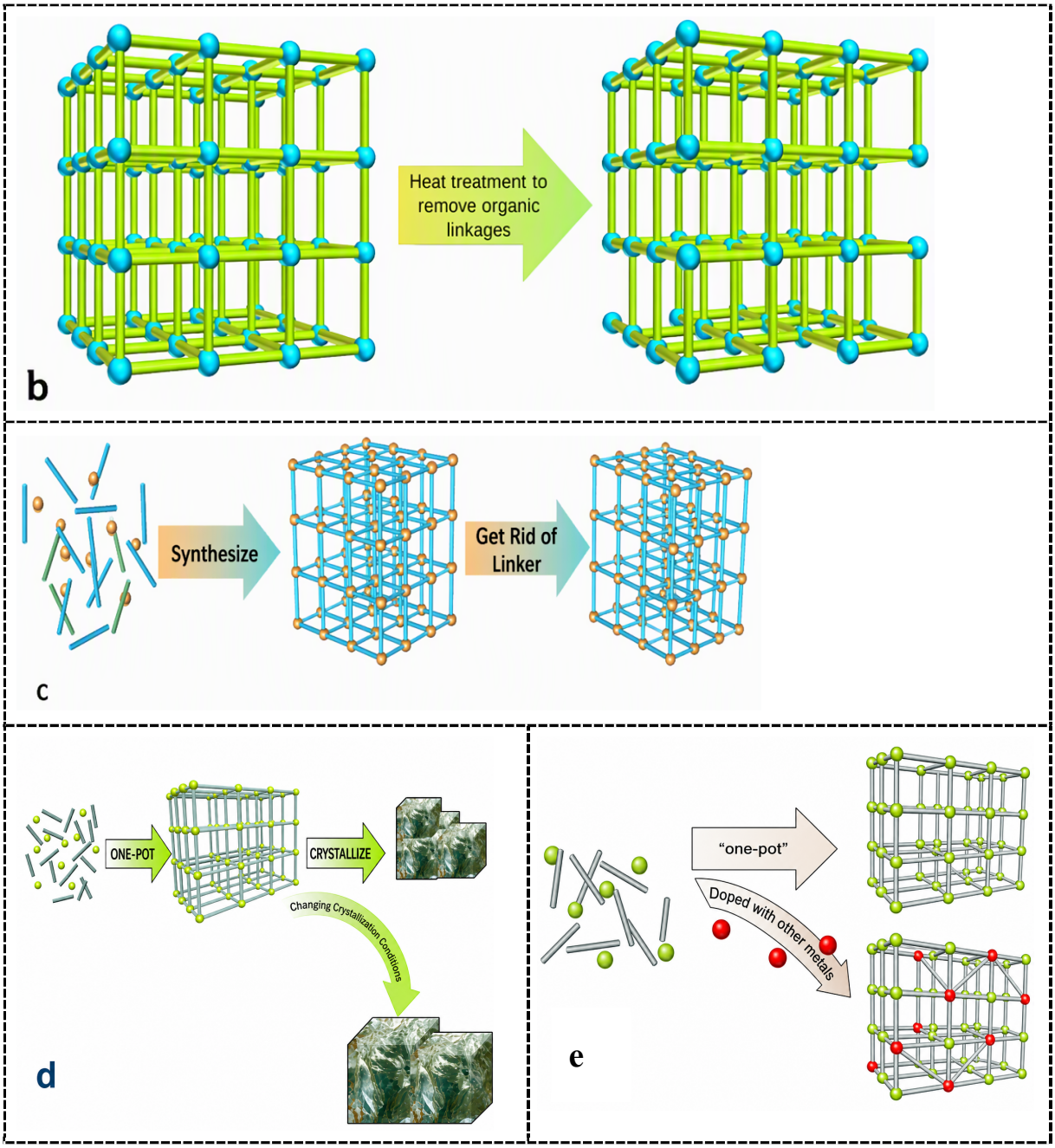


Figure 1. Schematic illustration of the three principal modification strategies for MOFs. (**a**) Defect engineering via metal-ion deficiency. (**b**) Defect engineering via thermal treatment. (**c**) Defect engineering via transient doping. (**d**) Modulator-assisted crystal engineering. (**e**) Metal-ion doping. (**f**) Functionalization.

3.2. Defect Engineering

Defect engineering is employed to intentionally create imperfections in MOFs structures, which can modulate their electronic properties, enhance catalytic activity, and introduce additional active sites. The following sections detail the introduction of such defects and their resulting impacts. Defect engineering refers to the deliberate creation and control of defects in materials—by varying defect types and densities—to tailor physical, chemical, electronic, and magnetic properties for specific functional applications [67]. Defects can be engineered at atomic, microstructural, and meso-macro scales [18]. In MOFs, defect engineering occurs primarily at the molecular level, and to a lesser extent, at the microstructural leve. These defects may include doping defects [68], topological defects [69], vacancy defects [70], etc., all of which play significant roles in materials science and physics. By introducing specific defect types, the physicochemical properties of MOFs can be modulated to improve performance. Defect engineering strategies in MOFs are broadly classified into two categories: modification of the MOF as a whole [71] and modification of MOFs components [72].

Component-level modification via defect engineering is achieved through two main approaches: altering the metal ions or metal clusters [73], and modifying the organic linkers [74]. Reducing the number of metal ions or clusters can increase the number of unbonded empty electron orbitals, thereby changing the morpho-structural properties of the MOF. Techniques such as thermal vibration or electron irradiation can induce vacancy formation by displacing metal ions or clusters from their original topological positions (Figure 1a). This process generates additional active sites, thereby enhancing the catalytic capability. Simultaneously, these vacancies may distort the MOF's topological structure and affect its physicochemical properties—such as electrical conductivity, mechanical strength, and durability.

The influence of defects on MOF performance is governed not only by their type but also by their concentration and distribution [18]. Defects in MOFs can be broadly categorized into metal-ion vacancies, linker vacancies, topological defects, and doping defects [67]. Metal-ion vacancies create coordinatively unsaturated metal sites (CUS) that can serve as Lewis acid sites for adsorption or catalysis. Linker vacancies increase porosity and may expose additional metal sites, but they also reduce the connectivity of the framework. Topological defects, such as missing clusters or struts, can alter pore architecture and mass-transport pathways, while doping defects arise from the intentional incorporation of heteroatoms or metal ions into the framework.

Accurate characterization of defect type, concentration, and distribution is therefore essential for establishing structure–property relationships. Electron paramagnetic resonance (EPR) is widely used to detect unpaired electrons associated with oxygen vacancies and metal-centered defects, providing direct evidence of defect existence and a qualitative measure of relative concentration. X-ray photoelectron spectroscopy (XPS) indirectly probes defect formation through changes in metal valence states (e.g., Ce^{3+}/Ce^{4+}, Ti^{3+}/Ti^{4+}) and oxygen vacancy-related O 1s components [63]. Raman spectroscopy offers a quantitative route via characteristic peak intensity ratios, such as the I(D)/I(F_2g) ratio for oxygen vacancies in certain metal oxides and MOF-derived materials [75]. X-ray diffraction (XRD) can reveal lattice strain, peak broadening, and crystallite size changes that accompany defect formation [76]. More directly, positron annihilation lifetime spectroscopy (PALS) can detect vacancy-type defects and provide information on their size and concentration. Combining these techniques is necessary because no single method can fully capture defect type, concentration, and spatial distribution [18].

Importantly, an increase in defect density does not automatically translate into improved performance. While moderate defect concentrations can enhance catalytic activity and adsorption capacity by increasing the number of active sites and improving pore accessibility, excessive defects often compromise the structural integrity of the framework [73]. High defect densities can lead to reduced crystallinity, framework collapse, and decreased chemical and thermal stability [67,77]. In adsorption, over-defective MOFs may exhibit reduced selectivity because the original pore architecture is disrupted, and competitive adsorption of interfering species can dominate [72]. In catalysis, excessive defects may act as recombination centers for charge carriers, lowering quantum efficiency in photocatalytic systems, or may promote metal-ion leaching, leading to deactivation and secondary pollution [78,79]. Therefore, an optimal "defect concentration window" exists for a given application, and this window must be determined empirically and rationalized through mechanistic studies. Recent work has begun to quantify this trade-off. For example, Farzaneh Rouhani and Mahsa Ghiasvand demonstrated that a moderate degree of linker deficiency in UiO-66 enhanced phosphate adsorption, whereas further defect introduction reduced both capacity and stability [80]. Similarly, while oxygen vacancies in a bimetallic MOF improved photocatalytic activity at low concentrations, higher vacancy densities increased charge recombination and decreased performance [75,78]. These findings underscore the need to report defect concentrations quantitatively and to correlate them with performance metrics, rather than assuming a monotonic benefit.

Organic linkers typically contain donor atoms (e.g., oxygen, nitrogen, sulfur) that provide lone pair electrons. Metal ions, acting as electron-pair acceptors, possess empty valence orbitals. Coordination bonds form when donor atoms donate electron pairs into these empty orbitals [81]. For instance, linkers with fewer oxygen atoms exhibit reduced connectivity to metal sites. Replacing linkers containing more oxygen atoms with those containing fewer can thus increase the number of empty electron orbitals on the metal ions. Wu et al. replaced 2,5-dioxo-1,4-benzenedicarboxylic acid (DOBDC, 6 O atoms) with fragmented linkers containing two to five oxygen atoms—such as 2-hydroxyterephthalic acid (BDC-OH), benzene dicarboxylic acid (BDC), 2,5-dihydroxybenzoic acid (DOBC), salicylic acid (BC-OH), and benzoic acid (BC)—resulting in MOFs with higher porosity and pore volume due to increased linker deficiency.

Defects [82] can also be introduced by using multiple linkers during synthesis. The interplay among different linkers can create additional electronic active sites and increase pore volume and porosity. For example, Han et al. incorporated BDC during the synthesis of Cu-MOF-2-NDC to obtain MTV-MOF-2 (C_4H_4), which exhibited a specific surface area of 94 m^2/g—intermediate between those of Cu-MOF-2-NDC (12 m^2/g) and Cu-MOF-2-BDC—demonstrating improved control over MOF fabrication and offering a new strategy for tailored MOF synthesis [83].

Another notable approach involves quasi-MOFs (Q-MOFs), a subclass of defect-engineered frameworks synthesized via controlled thermal treatment of pre-synthesized MOFs to partially remove organic linkers. This process introduces structural defects, enhances porosity, and exposes unsaturated metal sites (Figure 1b), thereby enhancing their adsorption performance [84,85]. For instance, Rouhani et al. prepared Q-M801-280 [80] and Q-MOF-303 [86] via thermal treatment. The heat treatment resulted in ligand loss in Q-M801-280, creating higher porosity and achieving a maximum adsorption capacity of 415 mg g^{-1} across a broad pH range of 3–11. Q-MOF-303, obtained through controlled pyrolysis in air, exhibited a maximum phosphate adsorption capacity of 488 mg g^{-1}. Additionally, X-ray photoelectron spectroscopy (XPS) peak fitting of the O1s region indicated that MOF-In_2O_3 possessed the highest oxygen vacancy density of 33.6%. Electron paramagnetic resonance (EPR) and photoluminescence (PL) spectroscopy further confirmed these findings, with the strongest EPR signal observed at 2580 G and enhanced PL peaks. This strategy underscores the potential of Q-MOFs as versatile platforms for advanced functional adsorption materials in energy and sustainability applications.

Alternatively, transient doping can be used during MOF synthesis—substances that readily complex with metal ions or clusters are temporarily introduced and later removed (Figure 1c), thereby altering MOF morphology and structure. This strategy often employs oxygen-containing compounds (e.g., phosphates or sulfates) that compete with native organic linkers for metal coordination. By adjusting synthesis conditions such as pH [87] and ion concentration [88], these dopants can partially displace organic ligands (e.g., carboxylates) to form mixed-ligand intermediates. Due to their weaker coordination strength (e.g., zirconium phosphate vs. zirconium carboxylate), these dopants are more likely to dissociate during subsequent treatments, thereby generating defects that enhance adsorption capacity.

Overall, modification of MOFs often involves controlling the crystallization process (Figure 1d), demonstrating promising applications in both adsorption and catalysis fields. Crystal size depends on nucleation and growth rates, which can be regulated using modulators to tailor particle size and specific surface area. Modulators are generally classified into three categories (Table 2): weak acids, surfactants, and strong coordinating agents. Weak acids (e.g., formic acid, acetic acid) protonate organic ligands, slowing nucleation and improving crystallinity and pore uniformity. For example, acetic acid-modified UiO-66 exhibits reduced defects and a high specific surface area (>1,200 m^2/g). The molar ratio of linker to metal (L/Zr) was determined by thermogravimetric analysis (TGA), yielding values between 0.77 and 0.98. This indicates varying degrees of linker deficiency, which is favorable for gas storage and adsorption [89]. Surfactants (e.g., cetyltrimethylammonium bromide (CTAB), polyvinylpyrrolidone (PVP)) inhibit agglomeration via micelle formation or steric hindrance, enabling precise size control. CTAB-assisted synthesis yields monodisperse ZIF-8 nanoparticles (<100 nm) for catalytic and membrane applications, while PVP-stabilized MIL-101(Cr) achieves surface areas exceeding 3000 m^2/g [90–92]. Simultaneously, Raman spectroscopy was employed to calculate the Ov/F_2g peak area ratio, thereby quantifying the oxygen vacancy concentration in the material. Additionally, XRD and XPS analyses were performed, which revealed changes in lattice constants and an imbalance in the redox states of metal ions, further confirming variations in oxygen vacancies. Strong coordinating agents (e.g., trifluoroacetic acid, pyridine) tightly bind metal ions, delaying nucleation to produce ultrasmall nanoparticles (<50 nm). TFA-modulated HKUST-1 nanoparticles (<20 nm) exhibit high catalytic activity in oxidation reactions, and pyridine-modulated ZIF-8 allows tunable hydrophobicity for separation membranes [93,94]. These modulator strategies address key challenges in crystallinity, dispersion, and nanoscale engineering, advancing MOFs for applications in catalysis, environmental remediation, and energy storage. Future research should prioritize eco-friendly modulators and in situ characterization to improve synthesis scalability and functionality.

Table 2. Three types of modulators and their scope of application.

Typology	Examples	Principle	Ref.
Weak acid type	Formic acid, acetic acid, etc.	Reduction of coordination capacity by protonated ligands	[89]
Surfactant	N, N, N-trimethylhexadecan-1 CTAB, PVP	Limits particle agglomeration and reduces particle size	[90–92]
Strong allotropic agent	Trifluoroacetic acid, Pyridine, etc.	Strongly binds metal ions, significantly retards nucleation, and generates ultra-small MOF nanoparticles (<50 nm)	[93,94]

In summary, defect engineering modifies the morpho-structural properties of MOFs through two primary strategies: (1) adjusting the metal ions, metal clusters, and organic linkers to alter topology, pore size, porosity, and surface area, enabling selective adsorption and enhanced adsorption capacity; and (2) controlling the overall crystal size during crystallization to tailor specific surface area and meet application-specific requirements.

3.3. Metal Ion Doping

In addition to defect engineering, the incorporation of metal ions [95]—designing bimetallic or multimetallic MOFs (Figure 1e)—can further enhance porosity, pore volume, and the number of electron-rich active sites, thereby improving adsorption and catalytic performance [96]. Increasing more electronic sites may also bring more catalytic active sites [53], resulting in a significant increase in catalytic performance. Interactions between different metals can improve electron transfer efficiency through mechanisms such as hybridization of electronic orbitals [97] and the formation of heterojunctions [98,99], as illustrated in Figure 2. Transition metals [100] are commonly employed in the preparation of multimetallic MOFs due to their multiple empty electron orbitals, which enable the formation of stable coordination compounds with diverse ligands. The selection of metals also influences the material's stability. Introducing suitable new metal ions or clusters (as summarized in Table 3) into the MOFs structure introduces metal nodes with distinct electronic configurations, altering the local topology and ultimately modifying the morpho-structural properties of the resulting material.

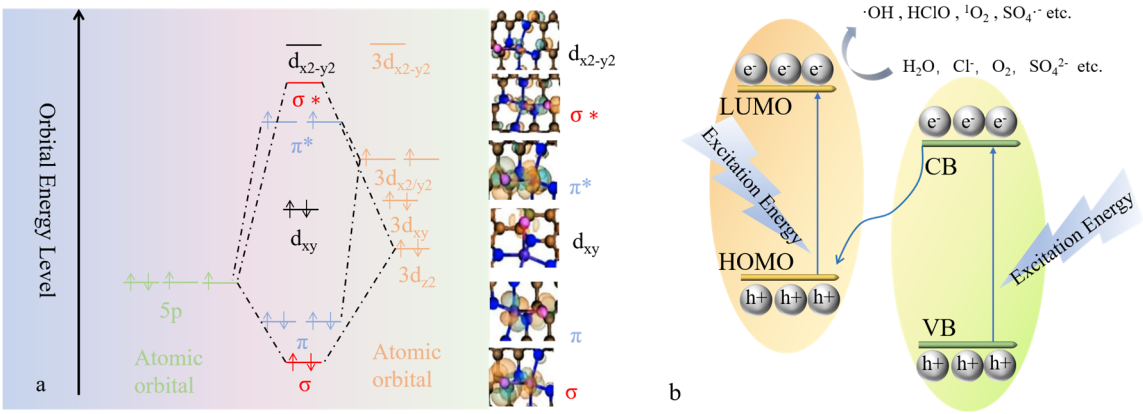


Figure 2. (**a**) Orbital hybridization between different metal centers. (**b**) Heterojunction formation and charge-transfer pathways.

For instance, Fe/Ce-MOFs [75] achieved photocatalytic nitrogen fixation via redox synergy between $Fe3^{+}$ and Ce^{4+}/Ce^{3+}, yielding an NH_4^+ production rate of 299—μmol·L^{-1}·h^{-1}. Meanwhile, the intensity ratio of I(D)/I(F_2g) from Raman spectroscopy was calculated to represent the relative concentration of oxygen defects, and XPS analysis was employed to indirectly confirm the presence of defects. This high activity arises from efficient nitrogen molecule activation at the bimetallic sites, facilitated by enhanced charge separation. Similarly, phosphorized ZIF-67 (NiCo) [53] exhibited improved methanol oxidation reaction (MOR) performance with a current density of 170 mA cm^{-2} at 1.54 V, where Ni provides catalytic activity and Co optimizes intermediate adsorption energy while reducing catalyst poisoning. In adsorption applications, MOF-74 (Mn-Ni) [96] demonstrated an iodine adsorption capacity of 219 mg g^{-1} through a redox cycle involving Mn^{2+}/Mn^{3+} and Ni^{2+}, enabling chemical reduction of iodine. Likewise, La/Ca-BTC [97] utilized the strong Lewis acidity of La^{3+} and the electrostatic interactions of Ca^{2+} to achieve a phosphate adsorption capacity of 101.01 mg P/g, with orbital hybridization further enhancing binding stability. Although MOFs exhibit excellent tunable performance in phosphate adsorption through defect engineering and metal doping, their synthesis often involves noble metals and organic ligands, resulting in high costs. In contrast, the preparation of adsorbents from agricultural or food industry waste offers greater economic and environmental sustainability. For example, López-Bermúdez et al. recently reported a bio-adsorbent prepared by co-pyrolysis of eggshell and sacha inchi (*Plukenetia volubilis*) peel, which demonstrated notable phosphate adsorption capacity while utilizing waste-derived materials aligned with circular economy principles [101]. This suggests that while pursuing high-performance adsorption materials, attention should also be directed toward developing low-cost and sustainable adsorption systems.

Bimetallic modifications also optimize material properties through heterostructure construction—such as partial sulfidation of Zn-Cd-MOF [102]—or electronic modulation between metals, as exemplified by orbital hybridization in CoFe-THQ [103]. For example, redox complementarity in NH_2-MIL-88B (Cu/Fe) [104] enabled simultaneous hydrogen production (1563.96 μmol· g^{-1}·h^{-1}) and urea synthesis (23.14 μmol·g^{-1}·h^{-1}), while the Fe-Cu heterojunction in MIL-100 (Fe/Cu) [98] promoted H_2O_2 decomposition into reactive oxygen species, degrading 95% of methylene blue within 40 min. Synthesis methods (e.g., plasma-assisted synthesis [75], solvothermal method [102]) and post-modification strategies (e.g., phosphide [53], sulfide [104]) further fine-tune bimetallic dispersion and interfacial properties, underscoring the critical roles of metal pairing and preparation protocols in enhancing performance.

The impact of polymetallic modification on the stability and ion leaching of MOF materials is dialectical, with the key lying in the rational selection and functional positioning of metal ions. When doped metal ions (e.g., Ca^{2+}, which has a similar ionic radius to La^{3+}) are well-matched, they can form stable structures or play a "sacrificial protection" role. For instance, Ca^{2+} preferentially binds with humic acid, reducing La^{3+}leaching by over 90% and significantly enhancing environmental safety. Conversely, the introduction of mismatched or unstable ions can disrupt the crystal integrity, exacerbating metal leaching and structural collapse. Therefore, the essence of poly-metallic modification is to adopt a strategy of "protecting high-function ions with low-risk ions", which enables the controlled adjustment of structural stability while actively suppressing the release of harmful ions, thereby achieving synergistic enhancement of both performance and stability.

Table 3. Bimetallic and multimetallic synergistic strategies for MOF modification.

MoFs	Metal	Application	Effect	Methodologies	Principle	Ref.
Fe/Ce-MOFs	Fe/Ce	Photocatalytic nitrogen fixation	NH_4^+ generation rate up to 299 μmol·L^{-1}·h^{-1}	Ionomer-assisted synthesis	More metal sites	[75]
ZIF-67	Ni/Co	MOR	170 mA cm^{-2} at a potential of 1.54 V	Phosphating	More metal sites	[53]
MOF-74	Mn/Ni	Efficient adsorption of radioactive iodine	Iodine adsorption capacity up to 219 mg g^{-1}	Reflux method	More metal sites	[96]
La/Ca-BTC	La/Ca	Adsorption removal of phosphate (PO_4^{3-})	Maximum adsorption capacity is 101.01 mg P/g.	High-temperature calcination	Orbital hybridization	[97]
CoFe-THQ	Co/Fe	Oxygen Evolution Reaction (OER)	Current density of 10 mA cm^{-2} can be achieved with an overpotential of 247 mV	Ethylenediamine modulation of metal ions	Orbital hybridization	[103]
Ni-Co-MOF	Ni/Co	Supercapacitors (SCs)	High specific capacity (289.6 mA h g^{-1} @ 4 mA cm^{-2})	Ion exchange	Orbital hybridization	[100]
Zn-Cd-MOF	Zn/Cd	Photocatalytic hydrogen production	Hydrogen production rate up to 27.65 mmol g^{-1} ·h^{-1}	Partial vulcanization	Construct heterojunctions	[102]
NH_2-MIL-88B	Cu/Fe	Hydrogen production, urea	The rate of hydrogen production amounted to 1563.96 μmol g^{-1} ·h^{-1} and the rate of urea synthesis amounted to 23.14 μmol g^{-1} ·h^{-1}	Solvothermal	Construct heterojunctions	[104]
MIL-100	Fe/Cu	Degradation of organic pollutants	95% degradation efficiency of Methylene Blue (MB) in 40 min over 0.05 g L^{-1} catalyst and 5 mM H_2O_2	Solvothermal	Construct heterojunctions	[98]

In summary, the polymetallic synergy strategy significantly enhances the catalytic performance of metal–organic frameworks (MOFs) while also improving their selective adsorption capability. These approaches increase the density of coordinatively unsaturated sites (CUS), enabling efficient selective adsorption of target substances. Catalytically, π-d conjugated orbital hybridization between different metals lowers reaction barriers, while increased current densities enhance catalytic capacity. The design of heterojunctions broadens charge carrier pathways, leading to higher electron transfer efficiency. These improvements originate from synergistic mechanisms—including electronic orbital hybridization, topological modulation, and efficient charge separation at heterogeneous interfaces within multi-metal nodes—offering a new paradigm for the functional design of MOFs.

3.4. Functionalization

Although the morphology, structure, and functionality of MOFs have been changed in defect engineering by substituting different organic linkers with each other or by using multiple organic linkers for MOFs in different fields, by introducing polymetallic central sites to improve their catalytic properties, and by using modulators, similarly, the functionalization of ligands is an effective technique to change the physicochemical properties of MOFs. The presence of novel free functional groups on the linkers [105,106] (Figure 1f) significantly enhances the material's porosity, thereby improving adsorption performance. This advancement holds promise for meeting the specific requirements of MOFs in various application fields.

Despite their high porosity and exceptional surface area, MOFs often exhibit limited adsorption capacity for certain pollutants, particularly heavy metal ions. The introduction of free functional groups on linkers (as summarized in Table 4) offers a promising route to improve the adsorption performance of MOFs. Furthermore,

the introduction of functional groups also alters the scalability and stability of the material. Common functional groups include carboxyl, amino, and hydroxyl groups [107,108]. Among these, hydroxyl groups can provide a high density of electronegative sites, positively influencing both adsorption and catalytic behavior [109]. Functional groups critically enhance MOF performance by enabling tailored host—guest interactions. Carboxyl groups demonstrate exceptional versatility, facilitating applications from uranium adsorption in MIL-101-SMA-AO (synergizing with amidoxime groups via complexation) [110] to phenolic compound capture in UiO-66 through coordination [111]. Hydroxyl/epoxy groups in MOF-1,5,9 strengthen hydrogen bonding for enhanced hydrogen storage [65], while sulfonyl groups in Mn(II)-MOF promote Congo Red adsorption via electrostatic interactions and H-bonding [112].

Nitrogen-containing groups expand MOF utility in sensing and regulation. Amino or mercapto groups in Cu-ETTC MOF suppress ligand-to-metal charge transfer (LMCT), enabling sensitive biomarker detection [113], whereas cyanide groups in USTC-2,3 modulate CO_2 adsorption through functional group interconversion [1]. These functional groups, covalently bonded to the organic framework, achieve uniform distribution and generally exhibit high chemical and thermal stability comparable to the parent MOF. However, the presence of strong coordinating groups (such as additional carboxyl groups) during synthesis may interfere with framework formation, potentially leading to reproducibility issues in large-scale production. Pyrazolyl-carboxylic acid in $Ln(Hpzbc)_2(NO_3)$ provides multibinding sites for selective $Fe^{3+}/Cr_2O_7^{2-}$ sensing, and phosphonate/carboxylate groups in Cd-MOF formhydrogen—bonded fluorescent probes for pyridine detection [21].

Synergistic effects between multiple functional groups unlock advanced functionalities. PCN-224 combines carboxylic and fluorinated groups for selective adsorption of KA mixtures via bicarboxylic ligand synergy [114], while DABA-MOF utilizes amino-carboxyl multiligand centers to enhance supercapacitor performance [115]. MOF-808-SSBDC integrates sulfonate and carboxyl groups to lower proton conduction energy barriers [109], and Zn-MOF merges carboxylic/sulfonic acid groups to improve both luminescence and proton conductivity [116].

Environmental remediation applications also leverage functional group interactions. MOF-5 employs carboxyl/amino groups for PM2.5 removal via electrostatic polarization [117]. MOF-808-AA adsorbs moxifloxacin hydrochloride through strong H-bonding mediated by sulfonic/carboxylic acids [118], and MIL-82 detects Ag^+ ions via carboxyl group-derived active sites [119]. UiO-66 exploits hydroxyls/carboxyls/epoxides to construct nanochannels for gas-liquid separation.

These studies collectively underscore how strategic functionalization—whether single groups like carboxyl in Zr-mel-NH_4 for cation exchange [120] or combinations like sulfonic/carboxylic acids in Zn-MOF—dictates MOF efficacy across energy, environmental, and biomedical applications, emphasizing their design-driven adaptability.

The scalability and stability of materials before and after functionalization remain a key research focus. As illustrated by the cyano group transformation in USTC-2,3 [1], functional groups are covalently bonded to the organic framework, achieving uniform distribution. These groups typically exhibit chemical and thermal stability comparable to the parent MOF. However, during synthesis, the presence of strongly coordinating groups (e.g., additional carboxyl groups) may interfere with framework formation, leading to reproducibility challenges in large-scale production. When the initial MOF synthesis can be independently optimized and standardized, subsequent functionalization steps—such as amidation, coordination, or polymerization—are often modular in design. For example, grafting sulfonic acid and carboxyl groups onto the nodes of MOF-808 [118], or functionalizing MIL-101 [110] with polymer chains bearing carboxyl/amidoxime groups, are processes generally more amenable to scale-up compared to de novo ligand synthesis. However, stability in this context involves multiple dimensions. Chemical stability depends on the newly formed bonds (e.g., amide, coordination bonds), which, though generally robust, may undergo hydrolysis under harsh conditions. Structural stability is typically high as the core framework is preserved, although pore accessibility may be affected. For instance, grafting long polymer chains onto MIL-101-SMA-AO for uranium adsorption significantly enhanced adsorption capacity but reduced the BET specific surface area, highlighting a trade-off between functional group density and porosity.

In conclusion, functionalization remains a cornerstone of MOF engineering. Pre-syntheticmethods are ideal when precise control over the framework topology and uniform functionality are paramount, despite scalability limitations. Post-syntheticmethods, with their superior scalability and flexibility, are better suited for rapid prototyping, introducing complex functionalities, and large-scale production. Future advancements will likely involve hybrid strategies and a deeper mechanistic understanding of group synergy to unlock the next generation of high-performance, application-specific MOFs.

Overall, the modification strategies for MOFs primarily encompass three core directions: defect engineering, introduction of multi-metal sites, and side-group functionalization. The quantification of defect density relies mainly on spectroscopic and energy-spectral analyses. Raman spectroscopy reflects oxygen-vacancy concentration directly through characteristic peak intensity ratios (e.g., $I(D)/I(F_2g)$); X-ray photoelectron spectroscopy indirectly

characterizes defect formation via metal valence-state ratios (e.g., Ce^{3+}/Ce^{4+}); X-ray diffraction allows calculation of lattice strain and crystallite-size variations, indicating the degree of structural distortion. Furthermore, electron paramagnetic resonance can detect unpaired electrons, providing direct evidence of defect existence. Integrating multiple spectroscopic techniques enables systematic quantification of defect types, concentrations, and distribution. Defect engineering modulates the physicochemical properties of materials by introducing doping defects, topological defects, vacancy defects, and distortion defects, thereby enhancing material performance. This approach not only broadens the application scope of MOFs but also improves catalytic/adsorption performance and enables high-sensitivity detection capabilities. Among these strategies, metal-ion deficiency and selective organic-linker substitution can notably enhance catalytic performance, while adjusting synthesis conditions and altering metal ions can improve adsorption performance. Direct introduction of multi-metal sites significantly increases the number of active sites and further optimizes material properties through orbital hybridization and heterojunction formation—a strategy typically aimed at boosting catalytic performance. Functionalization modifications, particularly those involving oxygen-containing groups, can create high-density electronegative sites, effectively enhancing the adsorption capacity and selectivity of materials toward specific substances.

Table 4. Common functional groups in MOFs and their applications.

MoFs	Functional Group	Application	Principle	Ref.
MOF-1, 5, 9	Hydroxyl, epoxy, and carboxyl groups	Hydrogen storage	Enhanced interface interactions	[65]
Mn(II)-MOF	Carboxy and sulfonyl groups	Congo Red (CR) highly selective adsorption	Hydrogen bonding and electrostatic interactions	[112]
Cu-MOF	Carboxy, hydroxy, and epoxy groups	Fuel cell	Electrostatic attraction and coordination	[20]
MIL-101-SMA-AO	Carboxy and amidoxime groups	Uranium adsorption	Synergy between functional groups	[110]
ZIF-8	Carboxy, carbonyl	Enhanced oxygen reduction reaction	Synergistic pyridine nitrogen boosting activity	[121]
USTC-2, 3	Cyanide, carboxylic acid	CO_2 adsorption	Regulatory mechanisms of functional group conversions	[1]
Cu-ETTC MOF	Amino or mercapto	Sensitive sensor	Hinder the LMCT process	[113]
PCN-224	Carboxylic and fluorinated groups	Selectivity for KA (mixtures of cyclohexanone and cyclohexanol)	Bicarboxylic ligand synergy	[114]
Cu-MOF	Amino group	Hepatitis B Infection Biomarkers Testing	Ligand interaction	[66]
Cd-MOF	Phosphonates and carboxylates	Selective fluorescent probes for pyridine detection	Hydrogen bond interaction	[21]
MOF-808-SSBDC	Sulfonate groups and carboxyl groups	Enhanced proton conductivity	Lowering the proton conduction energy barrier	[109]
MIL-53(AI)-NH_2	Nitrogen atom, carboxyl group, phosphite group	Uranium (U) adsorption	Surface complexation	[122]
DABA-MOF	Amino and carboxyl groups	Supercapacitor	Multiligand active center	[115]
UiO-66	Carboxyl group	Adsorption of phenolic acid compounds	Coordination	[111]
Zr–mel–NH_4	Carboxyl group	Reversible exchange of monovalent cations	Formation of uniform nanopores	[120]
MOF-5	Carboxy, amino	PM2.5 removal	Electrostatic interactions and polarization	[117]
Zn-MOF	Carboxylic acid, sulfonic acid group	Excellent luminescence and proton conductivity	Enhance proton conduction	[116]
MOF-808-AA	Sulfonic acid and carboxylic acid	Moxifloxacin hydrochloride adsorption	Strong bond interaction	[118]
MIL-82	Carboxyl group	Detection Ag	More active sites	[119]

3.5. Quantitative Comparison of Modification Strategies

The three modification strategies—defect engineering, metal-ion doping, and functionalization—each impart distinct performance trends across MOF applications, and their relative merits can now be assessed quantitatively.

(1) Activity

Defect engineering primarily enhances activity by increasing coordinatively unsaturated metal sites (CUS) and improving pore accessibility. Chloride-assisted defect engineering in Mg-MOF-74 increased the isosteric heat of CO_2 adsorption from 36 to 46 kJ mol^{-1} and raised ambient-pressure CO_2 uptake by ~15% [123]. Defective Zr-MOFs achieved maximum adsorption capacities of 661.7 mg g^{-1} for Eosin Y and 532.4 mg g^{-1} for methyl orange, maintaining high capacity after four regeneration cycles [124]. Quasi-HKUST-1 obtained by controlled thermal treatment showed a tenfold increase in Congo red capacity (715 vs. ~71 mg g^{-1}) [125]. However, excessive defects can suppress performance: solvent-derived formate defects in MOF-74 partially eliminated open metal sites and decreased N_2 and CO_2 adsorption with increasing defect concentration [126].

Metal-ion doping excels in boosting catalytic activity through multi-metal synergy. Co-, Ni-, and Cu-doped Zn-MOFs exhibited esterase activities of 0.47, 0.56, and 0.39 U/mg, respectively, versus 0.28 U/mg for pristine Zn-MOF—enhancements of 67.9%, 100.0%, and 40.0%. Optimal performance occurred at intermediate doping levels (Ni 50%, Co 75%), revealing a non-monotonic doping window [127]. In OER, bimetallic Mn–Co BTC MOFs showed 25% higher AC conductivity than monometallic analogues and achieved an overpotential of 359 mV at 10 mA cm^{-2} [128]. Fe/Ce-MOFs reached an NH_4^+ production rate of 299 μmol L^{-1} h^{-1} via Fe^{3+}/Ce^{4+} redox synergy [75].

Functionalization, especially with carboxyl, amino, or sulfonyl groups, enhances selective adsorption. Grafting a bulky diamine onto MIL-101 increased CO_2/N_2 selectivity ~3-fold versus a non-bulky diamine, achieving CO_2 capacity >1 mmol g^{-1} and CO_2/N_2 selectivity >100 at 100 kPa and 298 K [129]. Thiol-amino bifunctional UiO-66 membranes reached an ARU capacity of 111.14 mg g^{-1} with a separation factor $\alpha = 51.84$ [130].

(2) Selectivity

Defect engineering enhances selectivity mainly through hierarchical pores and stronger local binding. Defective Mg-MOF-74 showed ~20-fold higher CO_2/N_2 selectivity than the pristine material, attributed to stronger sites and faster mass transfer [123]. Aperture narrowing alone (fluorinated DMOF) raised CO_2/N_2 selectivity from 8.4 to 14.8, a smaller gain [123]. Functionalization offers superior molecular recognition: bulky diamine-grafted MIL-101 exceeded CO_2/N_2 selectivity of 100, outperforming most alkyl-amine-modified MOFs [129]. However, added functional groups reduce flux while increasing separation factor; excessive loading lowers capacity by crowding pore windows [131].

(3) Stability

Metal-ion doping often enhances stability. Cu-doped ZIF-8 remained reusable for at least three cycles without significant leaching or efficiency loss [132]. Cu(I)-MOF-808 retained 99.2% of its oxidative desulfurization performance after 12 cycles without framework collapse. In contrast, defect engineering can compromise stability: mesoporous MOF-808 collapses on cycling, and defects reduce mechanical stability and hydrophobicity [133]. Functionalization can enhance or reduce stability. Hydrophobic groups improved chemical stability, with BUT-155 stable in boiling water and pH 4–10 [21]. However, grafting long polymer chains onto MIL-101 enhanced capacity but reduced BET area, showing a trade-off between functional density and porosity.

(4) Scalability

Scalability remains challenging for all three strategies. Modulator-assisted defect engineering is compatible with existing MOF synthesis, but precise defect control is difficult to reproduce at scale [133]. One-pot metal-ion doping is relatively straightforward, but uniform metal distribution at production scale requires careful control of mixing and kinetics [132]. Post-synthetic functionalization offers high flexibility; spray drying has produced 50–100 kg/day of modified MOF, versus 0.5–2 kg/day for batch solvothermal post-synthetic modification [131]. However, extra steps increase cost, and strongly coordinating groups can interfere with framework formation, causing reproducibility issues.

(5) Limitations

Defect engineering: excessive defects reduce crystallinity and stability, may act as charge recombination centers, and are difficult to characterize reproducibly [133]. Metal-ion doping: metal leaching under acidic or oxidative conditions causes deactivation and secondary pollution; optimal doping ratio must be found empirically; mismatched ions disrupt crystal integrity [132]. Functionalization: pore blockage and reduced accessible area are common; strongly coordinating groups interfere with synthesis; extra steps increase cost and reduce scalability [131].

4. Applications in Environmental Remediation

MOFs have emerged as cutting-edge materials for cross-disciplinary applications, owing to their highly designable pore structures, ultrahigh specific surface areas, and tunable functionality. Their primary applications in water treatment include pollutant adsorption, water quality monitoring, and catalytic degradation, as illustrated in Figure 3. In adsorption, MOFs enable efficient capture of pollutants such as heavy metal ions through synergistic physicochemical mechanisms. In separation processes, their precise pore-size sieving and tailored surface chemistry significantly reduce the energy consumption of industrial separations. In sensing and detection, luminescent MOFs can identify trace pollutants with sensitivity far exceeding conventional methods. In catalysis, performance is enhanced by leveraging abundant metal active sites and cooperative interactions between metal centers.

Despite challenges related to humidity/thermal stability and scaling costs, MOFs are transitioning from laboratory research to broad applications—including carbon neutrality and precision medicine—through strategies such as framework stabilization with high-valency metal nodes (e.g., Zr, Al), machine learning-assisted design, and advances in green synthesis technologies. Consequently, MOFs are increasingly serving as core platforms enabling the "molecular engineering" paradigm.

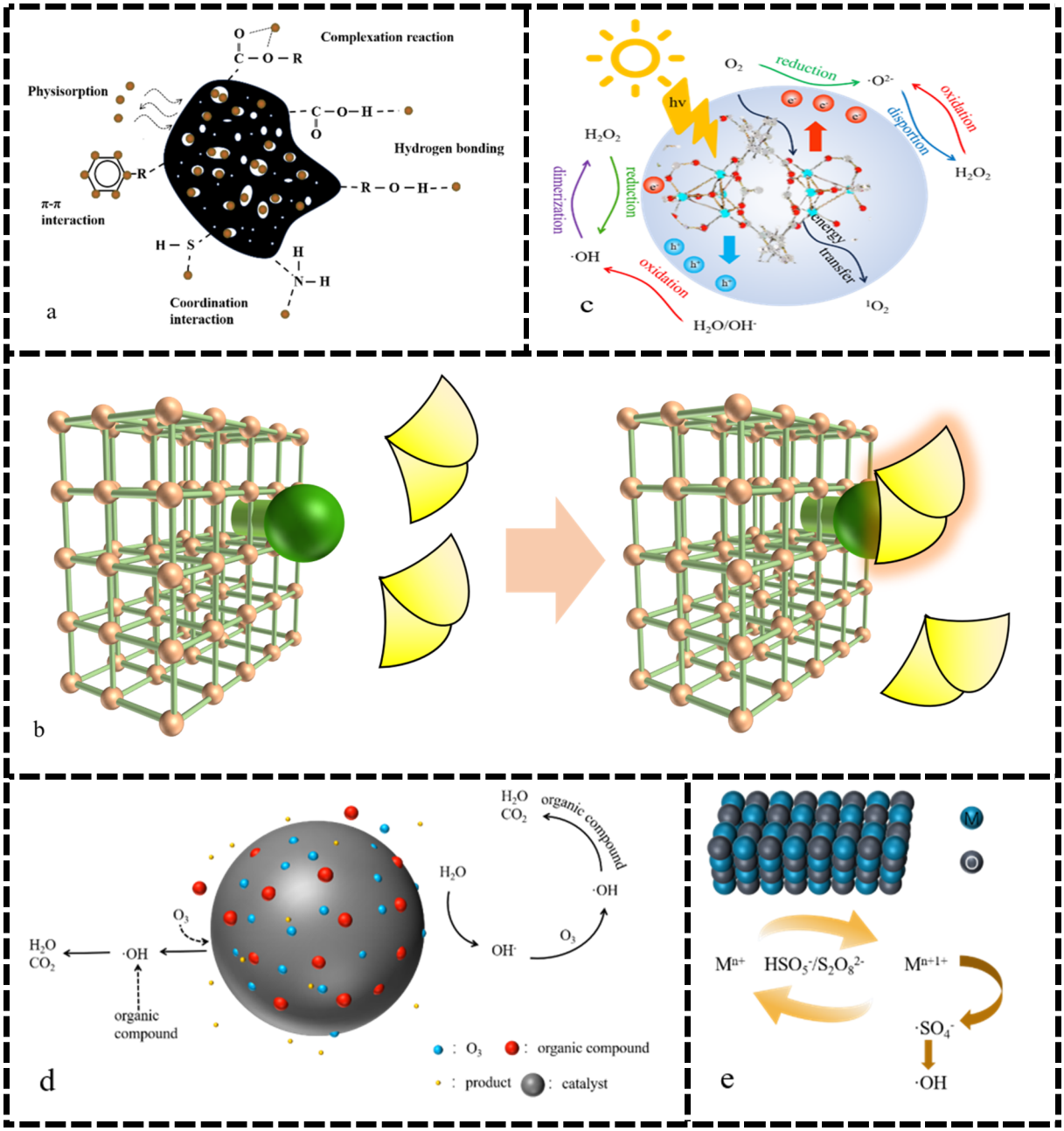


Figure 3. Applications of MOFs in water treatment: (**a**) adsorption, (**b**) molecular probing/sensing, (**c**) photocatalysis, (**d**) ozone catalysis, and (**e**) peroxymonosulfate (PMS) activation.

4.1. Adsorption of Pollutants

MOFs are widely employed for the adsorption and removal of various pollutants [2]—including heavy metal ions [134], acidic ions [135], and fuels [136]—because of their high porosity, adjustable pore structure, large specific surface area, abundant active sites, and ease of surface modification, as illustrated in Figure 3a. Enhancing the adsorption capacity of MOFs typically involves increasing their specificity toward target pollutants by modulating porosity and specific surface area, as well as through post-synthetic modification to introduce specific functional groups. To achieve these enhancements, various modification strategies—such as thermal treatment, the use of modulators to control crystallite size, and post-synthetic functionalization—are commonly employed. For instance, modifying MOFs with formic acid has proven highly effective for CO_2 adsorption, where adjusting the concentration or acidity of the carboxylic acid fine-tunes the material's porosity and composition, as summarized in Table 5.

Table 5. MOF-based adsorbents for pollutant removal.

MOF	Application	Methodologies	Effect	Enhancement	Principle	Ref
NH_2-UiO-66	Selective adsorption and removal of lead ions (Pb (II))	Seignette salt (potassium sodium tart rate) induced defect method	The adsorption capacity of Pb (II) amounted to 186.14 mg g^{-1}	34.2×	Formation of Zr vacancies and unsaturated ligand oxygen sites (Zr-OH).	[134]
HKUST-1	Adsorption of nitrogen (N_2)	Inorganic salt additives modulate crystal morphology and size	Evolution of continuous morphology from cubes to octahedra	-	Inhibition of crystal growth unit generation	[137]
La-MOFs	Efficient removal of pentavalent antimony (Sb(V))	Ligand position regulation	Sb(V) adsorption capacity up to 896.5 mg g^{-1}	-	Tuning the pore structure and active site distribution of MOFs	[138]
MOF-303	Phosphate removal	Pyrolytic partial deligandization	Maximum adsorption capacity up to 488 mg g^{-1}	25×	Pyrolytic partial removal of the ligand results in the formation of a large number of unsaturated Al^{3+} sites	[86]
MOF-808	Highly efficient phosphate removal	Ferric nitrate conditioning	Maximum adsorption capacity up to 305.5 mg g^{-1}	17% increase	Formation of defects and exposure of more unsaturated Zr sites	[71]

In the context of heavy metal ion removal, NH_2-UiO-66 exhibits outstanding selectivity and adsorption capacity for Pb(II) ions, with a maximum uptake of 186.14 mg g^{-1}. This represents a significant enhancement, being approximately 1.5–4 times higher than commonly used commercial activated carbons for Pb(II) (typical capacities 40–120 mg g^{-1}) and a 34.2-fold improvement over the pristine MOF material [134]. This enhancement is achieved via the Seignette salt (potassium sodium tartrate)-induced defect method, which generates Zr vacancies and unsaturated coordination oxygen sites (Zr-OH), providing abundant active sites for Pb (II) binding. Another notable example is La-MOFs, which achieve an impressive Sb(V) adsorption capacity of 896.5 mg g^{-1} through ligand position modulation—a strategy that fine-tunes pore structure and active site distribution to optimize adsorption performance [138]. This capacity vastly exceeds that of conventional adsorbents like iron-based oxides or activated alumina for antimony removal (typically <200 mg g^{-1}), underscoring the superior potential of defect-engineered MOFs. These results underscore the effectiveness of defect engineering in developing MOFs for environmental remediation, particularly for toxic heavy metal removal.

For phosphate adsorption, MOF-303 and MOF-808 demonstrate exceptional performance. MOF-303 achieves a maximum phosphate adsorption capacity of 488 mg g^{-1}—a 25-fold increase—through partial ligand removal via pyrolysis, which generates a high density of unsaturated Al^{3+} sites [86]. This value is notably higher than those of widely applied industrial adsorbents such as activated alumina (20–40 mg g^{-1}) and lanthanum-based materials (100–200 mg g^{-1}). Similarly, MOF-808 exhibits a phosphate adsorption capacity of 305.5 mg g^{-1} (a 17% improvement over its optimized baseline) using the nitric acid modulation method, where defects are introduced to expose additional unsaturated Zr sites [71]. These studies highlight the critical role of defect generation in enhancing the affinity and capacity of MOFs for anion removal, offering promising solutions for water purification.

The table also includes an example beyond CO_2 capture: HKUST-1 applied to nitrogen (N_2) adsorption. Using an inorganic salt additive-mediated method to control crystal morphology and size, continuous morphological evolution from cubic to octahedral structures was achieved, although specific adsorption performance was not quantified [137]. This example illustrates the broader potential of MOF modification techniques in tailoring crystal growth and morphology for specific applications.

In contrast to synthetic MOFs, natural adsorbents such as nano humic acid (NHA) [139,140]and chitinous materials[141] offer sustainable alternatives for environmental remediation. NHA exhibits dual-function

adsorption for heavy metals and nitrogen in soil (e.g., 76.1% Cu removal in 30 days), attributed to its nanoscale structure and functional groups like sulfonic and amino moieties. Similarly, chitosan derived from crustacean waste achieves >90% removal of transition and heavy metals (e.g., Cu, Pb) through abundant amino groups, albeit with lower specific capacity than MOFs. While MOFs excel in tailored porosity and ultrahigh uptake for targeted ions (e.g., 186.14 mg g^{-1} for Pb(II)), natural materials provide cost-effective, biocompatible solutions for complex matrices like soil and wastewater. Both systems underscore the role of surface functionalization and nanoscale design in enhancing adsorption, suggesting potential synergies in hybrid remediation strategies.

4.2. Pollutant detection

Molecular probes [142] are functional molecules capable of specifically recognizing and binding to target molecules while generating readily detectable signals, playing a pivotal role across numerous scientific fields. A typical molecular probe consists of a recognition group and a signal reporter group. As summarized in Table 6, MOF materials are applied in molecular probes primarily in two forms: one as carriers for molecular probes [143,144] as shown in Figure 3b, where fluorescent dyes are encapsulated within or grafted onto MOFs, enhancing detection intensity by increasing quantum yield through a spatial confinement effect; the other involves using MOF-derived porous carbon materials as electrode modification layers in electrochemical sensors [145], where their high electrical conductivity and active-site density significantly amplify current response and improve electrical signal detection.

MOFs have emerged as highly versatile materials in environmental monitoring, particularly for detecting water contaminants. Their tunable porosity, high surface area, and ease of functionalization make them ideal platforms for designing sensitive and selective sensors. Recent modifications of MOFs have substantially enhanced their detection performance, enabling applications in water treatment for identifying trace-level pollutants.

Functionalization of MOFs with specific recognition groups has greatly improved their selectivity. For instance, incorporating boronic acid groups into Eu-MOFs enables specific recognition of diol-containing molecules such as dopamine, allowing ratiometric fluorescence detection with a limit as low as 0.015 μM [146]. Similarly, amino-functionalized UiO-66-NH_2 exhibits strong affinity toward formaldehyde, facilitating its detection via fluorescence quenching within the range of 10–100 ppm [147]. These examples demonstrate how targeted functionalization can tailor MOFs for detecting specific organic contaminants in water. However, the long-term stability of these functionalized MOFs in aqueous environments, especially under varying pH, ionic strength, and in the presence of competing species, requires further evaluation for sustained field applications.

MOFs also serve as effective carriers for fluorescent probes, amplifying their sensing performance. For example, a Zn-MOF encapsulated with RhB enables highly sensitive detection of Cr(VI) through fluorescence quenching, with a detection limit of 20.5 ppb [143]. Likewise, MOF-808 loaded with RhB can simultaneously detect dopamine and Fe^{3+} via static quenching, achieving nanomolar-level detection limits [148]. This carrier role not only enhances signal output but also protects probe molecules, potentially improving sensor stability and reusability. The encapsulation strategy can mitigate probe leaching and degradation, yet the robustness of the host-guest structure over multiple detection-regeneration cycles needs systematic assessment to ensure practical reusability.

Furthermore, composite structures such as Ni-MOF integrated with nitrogen-doped NCDs enable dual-mode detection: Fe^{3+} quenches fluorescence, while ascorbic acid restores it, allowing indirect monitoring of redox-active species [144]. Such systems illustrate the potential of MOF composites in developing multi-analyte sensing platforms for water quality assessment. A critical challenge for such multi-analyte detection in real water samples is maintaining high selectivity within complex matrices containing diverse interfering ions and organic matter.

MOF-76 employs terbium ions (Tb^{3+}) combined with surface molecular imprinting to detect chlorpyrifos pesticides with high sensitivity (3.29 ng mL^{-1} limit) by monitoring characteristic Tb^{3+} emission at 544 nm [149]. Another Eu-MOF system detects flunitrazepam through combined PET and IFE that quench the MOF's fluorescence (73 nm limit) [62]. While impressive sensitivity is achieved, the selectivity of these probes against structurally similar analogs in environmental samples, as well as the regeneration capability of the imprinted or functionalized sites, are key parameters demanding further investigation for reliable deployment.

In conclusion, the modification of MOFs through functionalization and encapsulation strategies significantly boosts their performance as optical sensors for water contaminants. Their ability to detect a wide range of pollutants—including heavy metals, neurotransmitters, pesticides, and pharmaceuticals—with high sensitivity and selectivity underscores their promising role in advancing water treatment and environmental monitoring technologies. To transition from laboratory proof-of-concept to field-deployable devices, future research must prioritize enhancing the long-term operational stability of MOF-based sensors, validating their selectivity in realistic, complex water matrices, and optimizing their reusability through efficient regeneration protocols.

Table 6. MOFs as molecular probes for pollutant detection.

MOF	Target Molecule	Application	Detection Range	Detection Limit	Molecular Identification	Preparation Method	Principle	Detection Methods	Ref.
Eu-MOF	Dopamine (DA)	Directly as a probe	0–500 μM	Down to 0.015 μM	Boronic acid group (-$B(OH)_2$)	Functionalization of boronic acid groups	Specific recognition of cis-diol structures by boronic acid groups	Ratiometric fluorescence sensing	[146]
MOF-177	Electron paramagnetic resonance (EPR) signal	Vector (epidemiology)	EPR signal linewidth increases, strength decreases	-	Paramagnetic metal fullerene ($Sc_3C_2@C_{80}$)	Encapsulation	Anisotropy, linewidth, and intensity variations of the EPR signal of $Sc_3C_2@C_{80}$ to quantify subject-object interactions	EPR	[145]
UiO-66-NH_2	Formaldehyde (HCHO)	Directly as a probe	10–100 ppm	Detection limit: 4 ppm	Amino functional group (-NH_2)	One-pot method	Molecule-specific interactions of the amino functional group (-NH_2) with formaldehyde	Fluorescence quenching effect	[147]
Zn-MOF	Hexavalent chromium (Cr (VI))	Vector (epidemiology)	0–100 ppm	20.5 ppb	Rhodamine B (RhB)	Encapsulation	Fluorescence burst induced by RhB-Zn-MOF with Cr(VI)	Fluorescence spectroscopy	[143]
Ni-MOF	Fe^{3+}	Directly as a probe	0.029–8.0 μg/mL	0.0098 μg/mL	Nitrogen-doped carbon quantum dots (NCDs)	One-step hydrothermal method	Formation of non-fluorescent ground-state complexes of Fe^{3+} with Ni-MOF-NCDs	Fluorescence burst	[144]
	Ascorbic acid (AA)		0.263–18.0 μg/mL	0.0876 μg/mL			AA reduces Fe^{3+} to Fe^{2+}, releasing fluorescence	Fluorescence recovery	
MOF-76	Chlorpyrifos (CP)	Fluorescent probe	10–1000 ng mL^{-1}	3.29 ng mL^{-1}	Tb^{3+}	Surface imprinting	Characteristic emission (544 nm) of Tb^{3+} to detect targets	Fluorescence spectroscopy	[149]
MOF-808	DA	Vector (epidemiology)	0–80 μM	60.25 nM	RhB	Hydrothermal	DA or Fe^{3+} binds to the MOF ligand to form a nonfluorescent ground-state complex	Fluorescence static burst	[148]
	Fe^{3+}		0–40 μM	48.34 nM					
Eu-MOF	Flunitrazepam	Fluorescent probe	0–800 μM	73 nM	Eu^{3+}	Solvent heat	Photoinduced electron transfer (PET) and internal filtration effect (IFE)	Fluorescence spectroscopy	[62]

4.3. Catalytic Applications

MOFs, as a new type of porous materials characterized by high specific surface area, tunable pore structures, and diverse active sites, have demonstrated unique advantages in catalysis in recent years—particularly in advanced oxidation processes such as ozone catalysis, electrocatalysis, photocatalysis, and peroxymonosulfate (PMS) activation. The synergistic interplay between metal nodes and organic ligands enables efficient electron transfer, radical generation, and pollutant adsorption, significantly enhancing catalytic reaction efficiency. Through functional modifications (e.g., metal doping, defect engineering) and composite design (e.g., coupling with semiconductors or carbon-based materials), the catalytic activity and stability of MOFs can be further optimized, offering innovative solutions for environmental remediation (e.g., pollutant degradation) and energy conversion (e.g., water splitting, CO_2 reduction). However, practical applications still face challenges related to structural stability, scalable synthesis, and in-depth mechanistic understanding. Future research should focus on precise synthesis and multifunctional integration to advance the comprehensive development of MOF-based catalytic systems.

4.3.1. Photocatalysis

In the field of photocatalytic environmental remediation, MOFs have emerged as highly promising materials due to their tunable structures, high surface areas, and tailorable active sites. As summarized in the provided Table 7, various MOFs exhibit outstanding performance in the degradation of organic pollutants and reduction of heavy metals under light irradiation [150]. The mechanism of action is shown in Figure 3c.

Table 7. MOF-based catalysts for photocatalytic degradation.

MOFs	Application	Modification method	Principle	Performance	Active Sites	Ref.
Zif-8	Sulfonamides degradation	Treatment	P-n heterojunction	98.5%	Zn	[151]
Ce-MOF	Cr degradation	Composite semiconductors	Type-II heterojunction	95.6%	Ce	[152]
MIL-88B(Fe)	MB degradation	Regulate the conditions of solvothermal synthesis	Unsaturated metal sites	98%	Fe	[153]
Cd-MOF	RhB, tetracycline (TC) degradation	MOF derivatization	Type-I heterojunction	RhB95%; TC90%	Cd	[154]
Ag@MOF-525	RhB, TC degradation	Nanoparticle loading	Schottky heterojunction	RhB91%; TC81%	Zr, Ag	[155]
Cu-MOF	RB degradation	Gamma irradiation	The introduced defect sites	81.3%	Cu	[156]
ZnFe-MOF/AgCl	Levofloxacin degradation	Heterogeneous hybrid junctions	Z-type heterojunction	90.33%	Zn, Fe	[157]
NH_2-MIL-88	MB, RhB, TC degradation	One-pot method of hydrothermal synthesis	Polymetallic sites	MB99.99%; RhB 90.1%; TC96.6%	Fe, Cu	[158]

The photocatalytic performance of MOFs is governed not by degradation efficiency alone but by the interplay of light absorption, charge separation, and surface reaction kinetics. In MOF-based photocatalysts, the metal nodes and organic linkers can act as independent chromophores, and charge transfer can occur via ligand-to-metal charge transfer (LMCT) or metal-to-ligand charge transfer (MLCT); functional groups such as amino or mercapto groups can suppress LMCT and thereby alter catalytic or sensing behavior [113]. However, the short lifetime of photogenerated electron–hole pairs in pristine MOFs often limits quantum efficiency. Modification strategies therefore aim to suppress charge recombination and promote interfacial charge transfer. For example, constructing Type-II heterojunctions between MOFs and semiconductors spatially separates electrons and holes, as in Ce-MOF-based composites [152], but the resulting redox potentials may be insufficient for certain reactions. In contrast, Z-scheme heterojunctions, such as ZnFe-MOF/AgCl [157], preserve strong redox ability while enhancing charge separation. Schottky junctions formed by loading metal nanoparticles (e.g., Ag@MOF-525) introduce an internal electric field that facilitates electron extraction and reduces recombination [155]. Defect engineering adds another dimension: defect sites introduced by gamma irradiation in Cu-MOF [156] can serve as adsorption and catalytic sites, but at high concentrations they may act as recombination centers. The dominant reactive oxygen species (ROS)—including ·OH, $\cdot O_2^-$, and h^+—should be identified by scavenger experiments and EPR rather than inferred from degradation trends; for example, EPR and PL spectroscopy have been used to confirm oxygen vacancies in

Fe/Ce-MOFs and Q-MOFs [75,80,86]. Importantly, the relationship between MOF structure and photocatalytic mechanism is often nonlinear; amino-functionalization can enhance visible-light absorption but may also alter band-edge positions and change the dominant ROS, as observed in NH_2-MIL-125(Ti) [159]. Therefore, mechanistic studies should combine transient absorption spectroscopy, photoluminescence, and electrochemical impedance spectroscopy to elucidate charge dynamics, rather than relying solely on degradation rate constants [75,150,158].

4.3.2. Ozone Catalysis

In ozone catalysis, MOFs function through three interrelated mechanisms: (i) adsorption and enrichment of ozone on the catalyst surface, (ii) electron transfer from the MOF to ozone, and (iii) generation of hydroxyl radicals (·OH) via surface hydroxyl groups or metal sites. The metal nodes—particularly those with multiple valence states (e.g., Co, Fe, Mn)—can activate ozone through Lewis acid–base interactions, while surface hydroxyl groups promote the decomposition of ozone into ·OH [160,161]. However, a critical limitation is that ozone is a strong oxidant that can attack the organic linkers of MOFs, leading to structural collapse and loss of catalytic activity. This trade-off between activity and stability is often overlooked. For example, ZIF-67 modified with FeOOH shows enhanced total organic carbon (TOC) removal but suffers from cobalt leaching and linker oxidation after repeated cycles [160]. Similarly, Mg-MOF-74 derived materials exhibit high chemical oxygen demand (COD) removal but may lose organic components under prolonged ozone exposure [3]. In contrast, the carbonized Fe/Cu/Zn-MOF system completely degrades ibuprofen within 30 min, producing 48 times more ·OH than conventional ozonation, which is attributed to Fe^{2+}-mediated Fenton-like reactions, H_2O_2 activation by the carbon matrix, and multi-metal electron cycling [161]. Therefore, the design of ozone-resistant MOFs requires either the use of oxidation-resistant linkers or the conversion of MOFs into more stable derivatives. Mechanistic studies should focus on identifying the active oxygen species and on quantifying the contribution of homogeneous vs. heterogeneous pathways; in situ Raman and EPR spectroscopy under ozone exposure can provide direct evidence of reactive intermediates and structural changes.

4.3.3. Persulfate Activation

In MOF-based Peroxodisulfate/Peroxodisulfate **(**PMS/PDS) activation, the debate between radical and non-radical pathways is central to understanding selectivity and efficiency (Table 8). Radical pathways involve the generation of SO_4^{-}· and ·OH through metal redox cycling (e.g., Fe^{3+}/Fe^{2+}, Co^{3+}/Co^{2+}), and the rate-limiting step is often the regeneration of the reduced metal state [162,163]. In contrast, non-radical pathways—such as singlet oxygen ($^1O_2$) generation, electron transfer from pollutants to the catalyst surface, or high-valent metal–oxo species—can dominate under certain conditions and offer advantages in terms of selectivity and resistance to background scavengers [164]. The prevailing pathway depends on the MOF's metal identity, coordination environment, defect density, and surface hydrophobicity. For example, Fe-MOF-CC@MoS_2 promotes both radical and non-radical pathways, with MoS_2 facilitating Fe^{3+}/Fe^{2+} cycling and $^1O_2$ generation. MOF-derived BFO further confirms the efficacy of iron redox chemistry, showing 95.5% naproxen degradation through Fe(III)/Fe(II)-activated PMS [165]. However, the relative contribution of each pathway is rarely quantified. Moreover, the stability of MOFs under oxidative conditions is a critical concern: PMS and PDS can attack organic linkers, leading to framework degradation and metal leaching, which reduces catalytic activity and may cause secondary pollution. Therefore, mechanistic studies should include quenching experiments, EPR spin-trapping, and electrochemical analysis to distinguish pathways, complemented by stability tests under relevant conditions. The design of oxidation-resistant linkers and protective coatings is essential for practical application [159,162].

Table 8. MOF-based catalysts for peroxymonosulfate (PMS) activation.

MOFs	Application	Modification Method	Principle	Performance	Active Sites	Ref.
MIL-100, MIL-88A	Degradation of organic pollutants in landfill leachate	High-temperature carbonization	Fe^{2+} on MOF surface activates H_2O_2 or $S_2O_8^{2-}$ to generate ·OH or SO_4^{-}· radicals	>90% COD removal	Fe	[162]
MIL-53(Fe) MIL-101(Fe) Fe_3O_4@MIL-101(Fe)	Degradation of emerging contaminants	Magnetic nanoparticle modification, metal doping	Metal nodes activate PS or PMS via electron transfer, generating SO_4^{-}· and HO· through chain reactions	>90% removal of Acid Orange	Fe	[163]
NH_2-MIL-125(Ti)	TC degradation	*In situ* growth, functionalization	Heterojunction charge separation	82.8% TC degradation	-NH_2,Ti	[159]

Table 8. *Cont.*

MOFs	Application	Modification Method	Principle	Performance	Active Sites	Ref.
Fe-MOF-CC@MoS_2	Degradation of TC, Ciprofloxacin (CIP), Nitrofurantoin (NFT), Sulfamethoxazole (SMX)	Hydrothermal carbonization	Fe^{3+}/Fe^{2+} activation over PMS to produce SO_4-, ·OH, $^1O_2$	Removal rates: TC 96.51%, CIP 92.30%, NFT 88.96%, SMX 80.76%	Fe, Mo	[164]
MOF-d BFO	Naproxen (NPX) degradation	High-temperature calcination	Fe (II)/Fe (III) cycling activates PMS to generate radicals (SO_4^{-}· and ·OH)	95.5% degradation efficiency	Fe	[165]

4.3.4. Electrocatalysis

Although electrocatalysis was not the primary focus of the original review, its mechanistic principles are closely related to the modification strategies discussed herein. In MOF-based electrocatalysts, the metal nodes serve as active sites, and their intrinsic activity is determined by the electronic structure, particularly the d-band center relative to the Fermi level. Coordination unsaturation—arising from defects or linker vacancies—creates open metal sites that can bind reaction intermediates more strongly. Metal-ion doping can tune the d-band center through orbital hybridization, optimizing the adsorption energies of intermediates such as *OH, *O, and *OOH in the oxygen evolution reaction (OER) and oxygen reduction reaction (ORR). For example, CoFe-THQ exploits orbital hybridization between Co and Fe to achieve an OER current density of 10 mA cm^{-2} at an overpotential of 247 mV [103], while Ni-Co-MOF benefits from orbital hybridization for high specific capacity [100]. In the methanol oxidation reaction (MOR), phosphorized ZIF-67 (NiCo) exhibits a current density of 170 mA cm^{-2} at 1.54 V, where Ni provides catalytic activity and Co optimizes intermediate adsorption energy while reducing catalyst poisoning [53]. Heterostructure formation with conductive materials improves charge transfer and prevents aggregation. However, MOFs often suffer from poor electrical conductivity and instability under electrochemical conditions, which limits their direct use as electrocatalysts. In many cases, MOFs are pyrolyzed to form MOF-derived carbon/metal composites, which inherit the porous structure but lose the molecular definition of the original framework. The mechanistic understanding of MOF-based electrocatalysis is further complicated by the dynamic reconstruction of the catalyst surface under operating potentials, which can convert metal nodes into oxyhydroxides that are the true active species. Therefore, operando X-ray absorption spectroscopy and Raman spectroscopy are essential to identify the real active phases. Future research should focus on designing conductive MOFs, stabilizing open metal sites, and establishing clear structure–activity relationships under reaction conditions.

4.4. Regeneration and Reusability

The practical viability of MOF-based materials depends not only on initial performance but also on regenerability and reuse over multiple cycles. This section compares regeneration methods, cycle stability, energy and reagent consumption, and structural integrity for both adsorption and catalysis.

Common methods include solvent washing (methanol, ethanol, acetone), pH-adjusted elution, thermal treatment, and emerging electrochemical or solar-light-triggered regeneration [166]. For ZIF adsorbents, NaOH, methanol, and ethanol are effective desorption agents. Ethanol elution enabled AlFu-PEI to retain >86% removal after five cycles with <15% capacity loss. Acidic or alkaline solutions are widely used for heavy-metal-loaded MOFs; De-UiO-66-NH_2 regenerated with 0.1 M HCl and 0.5 M NaOH maintained >90% phosphate and >85% Pb^{2+} removal after five cycles [167]. However, repeated acid/alkali exposure can degrade frameworks, with ZIF-8 losing up to 50% capacity after four cycles [168].

Reported stability varies widely. Al-CAU-60/PVF retained performance over seven water-triggered cycles, whereas zeolite 13X lost ~90% capacity after one cycle [169]. UiO-66-based materials generally show good reusability: De-UiO-66-NH_2 retained >85% Pb^{2+} and >90% phosphate removal after five cycles [167]; UiO-66@PVA beads maintained crystallinity over ten cycles [170]. Zr-DMSA retained ~63% capacity after ten cycles [171]. For ZIFs, RPZIF-8 kept ~78% Rhodamine B capacity after eight cycles, while ZIF-8 and Fe-ZIF-8 maintained 90% and 95% of Remazol Deep Black RGB capacity after three cycles [172]. In contrast, DUT-5 lost most diclofenac capacity in one regeneration (30.66 to 8.12 mg g^{-1}) [171]. A mini-review concluded that MOF-based systems generally show capacity losses below 10–15% after several cycles, especially composites and functionalized systems.

Thermal regeneration is energy-intensive. Temperature-swing adsorption at 150 °C requires 1875.66 kJ/kg, and pressure–vacuum swing adsorption consumes 1.79–2.14 MJ/kg CO_2 [10]. Pilot-scale MOF direct air capture achieved 1.6 kWh/kg CO_2 [173]. Solvent-based regeneration uses organic reagents but often operates at ambient

temperature. Solar-light-triggered regeneration and Joule heating are promising low-energy alternatives; solar-assisted biochar–MOF cycling showed <10% capacity loss after 50 cycles [174]. However, these methods remain laboratory-scale.

Post-regeneration integrity is assessed by XRD, BET, and SEM. UiO-66@PVA beads retained crystallinity over ten cycles [170]. In contrast, MIL-100(Fe) for Cr(VI) removal lost ~30% BET area after three alkaline regenerations, with efficiency dropping from 95% to 70% [168]. ZIF-8 for Cu^{2+}/Pb^{2+} underwent progressive amorphization upon acid regeneration, with 50% capacity loss after four cycles [168]. Zr-DMSA lost ~4.41% of its linkers in the first cycle [171]. Generally, high-valence metal nodes (Zr^{4+}, Cr^{3+}) resist regeneration-induced degradation better than low-valence nodes (Zn^{2+}, Cu^{2+}) [168].

For persulfate activation, BiOBr/MIL-100(Fe) showed only 14.48% degradation reduction after three cycles. MIL-53(Fe) exhibited good reusability at near-neutral pH. In photocatalysis, Ag/Ag_2O@MOF-808 had 0.417% Ag^+ leaching and >73% activity retention after four cycles, with XRD, FT-IR, SEM, and BET confirming integrity [175]. Cu-ZIF-9-ica showed no metal leaching during repeated methylene blue degradation [132]. However, metal leaching, structural collapse, and pore blockage remain common. Ni/MgO@C derived from bimetallic MOFs lost ~20% Ni, causing deactivation. Thus, future studies should report catalyst mass loss, metal ion release (ICP-OES/MS-ICP), and structural characterization after cycling.

Well-designed composites, highly crystalline frameworks, and high-valence metal nodes can achieve viable cycle stability, whereas unmodified frameworks with weak desorption or poor hydrolytic stability are unsuitable for reuse. Regeneration method choice must balance desorption efficiency against structural preservation; hybrid chemical–thermal strategies show potential. Future work should systematically report regeneration method, cycle number, capacity retention, energy/reagent consumption, and post-cycling characterization. Most studies remain batch-scale with few cycles; increased cycles, leaching tests, continuous-flow evaluation, and techno-economic analysis are needed for practical implementation.

5. Challenges and Future Perspectives

Despite the significant progress made in the field of MOFs, several challenges remain to be addressed for their widespread application in practical scenarios. Firstly, the long-term stability of MOFs under operational conditions, especially in harsh environments such as high temperatures or acidic/alkaline solutions, needs to be improved. Secondly, the scalability of MOF synthesis methods must be enhanced to meet the demand for large-scale production. Current synthesis techniques often suffer from low yields and high costs, which hinder their commercialization.

In-depth mechanistic studies are also crucial for fully understanding the behavior of MOFs in different applications. This knowledge will guide the rational design of new MOFs with enhanced properties and functionalities. Additionally, interdisciplinary collaborations are needed to leverage advances in materials science, chemistry, and engineering to push the boundaries of MOF research.

Future research should focus on developing more robust and scalable MOF materials through innovative synthesis methods and modification strategies. The integration of machine learning and artificial intelligence can also accelerate the discovery and optimization of new MOFs for specific applications. By addressing these challenges and leveraging ongoing technological advancements, MOFs have the potential to revolutionize various environmental and engineering fields, contributing to a more sustainable and cleaner future.

In conclusion, MOFs continue to be at the forefront of materials science research due to their unique properties and diverse applications. With ongoing efforts to improve their stability, scalability, and understanding of their reaction mechanisms, MOFs hold great promise for addressing global challenges related to energy, environment, and health.

6. Conclusions

This review has surveyed the significant progress in MOF modification strategies and their applications in water treatment from 2015 to 2025. While defect engineering, metal-ion doping, and functionalization have each demonstrated remarkable potential, the field now stands at a critical juncture where laboratory successes must be translated into practical technologies. To achieve this, future research should focus on the following priorities:

First, water-stable MOF design. Many high-performance MOFs suffer from hydrolysis or structural degradation in aqueous environments, particularly under acidic or alkaline conditions. Developing MOFs with high-valency metal nodes (e.g., Zr^{4+}, Al^{3+}, Ti^{4+}) or hydrophobic linkers, and employing protective encapsulation strategies, will be essential for long-term operation.

Second, machine learning-assisted discovery. The vast compositional and structural space of MOFs makes traditional trial-and-error approaches inefficient. Integrating machine learning with high-throughput experiments and computational screening can accelerate the identification of optimal MOFs for specific pollutants, predict stability under realistic conditions, and guide the design of multi-functional materials.

Third, in situ and operando characterization. A deeper understanding of defect dynamics, active site evolution, and degradation mechanisms requires advanced in situ techniques such as synchrotron-based X-ray absorption spectroscopy, environmental transmission electron microscopy, and operando Raman spectroscopy. These methods can reveal structure–property–mechanism relationships that are inaccessible to ex situ analysis.

Fourth, scalable and green synthesis. The gap between laboratory-scale synthesis and industrial production remains wide. Future efforts should focus on continuous-flow synthesis, mechanochemical methods, and the use of renewable or waste-derived linkers and metal sources. Cost analysis and life-cycle assessment should be integrated early in materials development.

Fifth, multi-strategy integration. Combining defect engineering, metal doping, and functionalization in a single MOF system—rather than treating them as separate approaches—can yield synergistic effects. For example, defect-rich bimetallic MOFs with grafted functional groups may simultaneously achieve high adsorption capacity, selective recognition, and robust catalytic activity.

Sixth, validation under realistic water matrices. Most reported studies use deionized water or simple aqueous solutions. Future research must evaluate MOF performance in the presence of competing ions, natural organic matter, and fluctuating pH and temperature, and should assess regeneration, long-term stability, and leaching of metal ions. Pilot-scale testing and techno-economic analysis will be critical for commercialization.

In summary, MOFs hold great promise for advancing water treatment technologies, but their translation from laboratory curiosities to practical solutions requires a concerted, interdisciplinary effort. By addressing the priorities outlined above, the research community can unlock the full potential of MOFs for sustainable environmental remediation.

Author Contributions

F.Y.: conceptualization, methodology, investigation, data curation, formal analysis, visualization, writing—original draft preparation, writing—review and editing. J.W.: investigation, data curation, formal analysis, visualization. X.L.: methodology, validation, investigation, data curation, writing—review and editing. H.L.: investigation, data curation, validation, visualization. Y.F.: conceptualization, methodology, supervision, project administration, funding acquisition, writing—review and editing. Y.Y.: conceptualization, methodology, supervision, project administration, writing—review and editing. All authors have read and agreed to the published version of the manuscript.

Funding

This work was funded by the funding program of 20 policies for universities in Jinan (202333071) and the Natural Science Foundation of Shandong Provincial, China (ZR2025MS817).

Institutional Review Board Statement

Not applicable. This review article did not involve studies with human participants or animals, and no ethical approval was required.

Informed Consent Statement

Not applicable. This study did not involve human participants, and no informed consent was required.

Data Availability Statement

No new data were generated or analyzed in this review. All data and information discussed are derived from previously published studies and are cited in the reference list. Therefore, data sharing is not applicable to this article.

Conflicts of Interest

The authors declare no conflict of interest.

Use of AI and AI-Assisted Technologies

During the preparation of this work, the authors used DeepSeek-V3-0324 to improve the language and readability of the manuscript. After using this tool, the authors reviewed and edited the content as needed and take full responsibility for the content of the published article.

References

1. Li, B.; Yan, Q.-Q.; Xu, Z.-Q.; et al. Tuning the interpenetration of metal–organic frameworks through changing ligand functionality: Effect on gas adsorption properties. *CrystEngComm* **2020**, *22*, 506–514. https://doi.org/10.1039/c9ce01309a.
2. Zhang, L.; Qu, Y.; Zhao, Y.; et al. Synthesis and Phosphate Removal of Ce/Mg-MOF-74. *Pol. J. Environ. Stud.* **2025**, *34*, 4915–4925. https://doi.org/10.15244/pjoes/190322.
3. Li, Y.; Zhang, Z.; Zhang, L.; et al. Preparation of metal organic frame derived MgO-porous carbon composite and its high catalytic activity in ozonation with excellent stability. *J. Taiwan Inst. Chem. Eng.* **2024**, *156*, 105339. https://doi.org/10.1016/j.jtice.2023.105339.
4. Ngo, T.C.Q.; Nguyen, T.N.D.; Chau, H.D.; et al. Evaluation of the Effect of Bimetallic Organic Framework M/Fe-MOF (M=Ni, Co) on the Removal of Congo Red Dye. *Pol. J. Environ. Stud.* **2023**, *32*, 1313–1322. https://doi.org/10.15244/pjoes/155874.
5. Raghav, S.; Chavda, V.; Yadav, A.; et al. Advanced MOF-based materials for adsorptive and photocatalytic removal of emerging organic pollutants from wastewater. *Appl. Mater. Today* **2025**, *46*, 102865. https://doi.org/10.1016/j.apmt.2025.102865.
6. Chavda, V.; Borah, P.; Thakar, M.; et al. Deep eutectic solvent engineered metal–organic frameworks (DES-MOFs): A green pathway toward next-gen advanced functional materials. *Chem. Eng. J.* **2026**, *545*, 179356. https://doi.org/10.1016/j.cej.2026.179356.
7. Raghav, S.; Chavda, V.; Thakar, M.; et al. A state-of-the-art review on Fe-based metal–organic frameworks (Fe-MOFs) for removal of hazardous dyes in aqueous environment: Mechanisms, modifications, and future prospects. *Desalination* **2026**, *631*, 120205. https://doi.org/10.1016/j.desal.2026.120205.
8. Yaghi, O.M.; Li, G.; Li, H. Selective binding and removal of guests in a microporous metal–organic framework. *Nature* **1995**, *378*, 703–706. https://doi.org/10.1038/378703a0.
9. Li, H.; Eddaoudi, M.; O'Keeffe, M.; et al. Design and synthesis of an exceptionally stable and highly porous metal-organic framework. *Nature* **1999**, *402*, 276–279. https://doi.org/10.1038/46248.
10. Feng, Y.; Yao, J. Tailoring the structure and function of metal organic framework by chemical etching for diverse applications. *Coord. Chem. Rev.* **2022**, *470*, 214699. https://doi.org/10.1016/j.ccr.2022.214699.
11. Beltrán, F.J.; Álvarez, P.M.; Gimeno, O. Graphene-Based Catalysts for Ozone Processes to Decontaminate Water. *Molecules* **2019**, *24*, 3438. https://doi.org/10.3390/molecules24193438.
12. Wang, J.; Zhuan, R. Degradation of antibiotics by advanced oxidation processes: An overview. *Sci. Total Environ.* **2020**, *701*, 135023. https://doi.org/10.1016/j.scitotenv.2019.135023.
13. Mukherjee, A.; Chakrabarty, S.; Kumari, N.; et al. Visible-Light-Mediated Electrocatalytic Activity in Reduced Graphene Oxide-Supported Bismuth Ferrite. *ACS Omega* **2018**, *3*, 5946–5957. https://doi.org/10.1021/acsomega.8b00708.
14. Hou, J.; He, X.; Zhang, S.; et al. Recent advances in cobalt-activated sulfate radical-based advanced oxidation processes for water remediation: A review. *Sci. Total Environ.* **2021**, *770*, 145311. https://doi.org/10.1016/j.scitotenv.2021.145311.
15. Wuttke, S.; Braig, S.; Preiß, T.; et al. MOF nanoparticles coated by lipid bilayers and their uptake by cancer cells. *Chem. Commun.* **2015**, *51*, 15752–15755. https://doi.org/10.1039/c5cc06767g.
16. Chávez, A.M.; Rey, A.; López, J.; et al. Critical aspects of the stability and catalytic activity of MIL-100(Fe) in different advanced oxidation processes. *Sep. Purif. Technol.* **2021**, *255*, 117660. https://doi.org/10.1016/j.seppur.2020.117660.
17. Payam, A.F.; Khalil, S.; Chakrabarti, S. Synthesis and Characterization of MOF-Derived Structures: Recent Advances and Future Perspectives. *Small* **2024**, *20*, 2310348. https://doi.org/10.1002/smll.202310348.
18. Xiang, W.; Zhang, Y.; Chen, Y.; et al. Synthesis, characterization and application of defective metal–organic frameworks: Current status and perspectives. *J. Mater. Chem. A* **2020**, *8*, 21526–21546. https://doi.org/10.1039/d0ta08009h.
19. Cheng, H. One-Pot Preparation of HCPT@IRMOF-3 Nanoparticles for pH-Responsive Anticancer Drug Delivery. *Molecules* **2023**, *28*, 7703. https://doi.org/10.3390/molecules28237703.
20. Sun, H.; Wang, K.-Z.; Yao, M.-R.; et al. Fabrication of ultrathin two-dimensional MOF nanosheets with cage-like cavities showing excellent adsorption for lead(II). *Inorg. Chem. Front.* **2023**, *10*, 6566–6577. https://doi.org/10.1039/d3qi01619f.
21. Wu, G.-M.; Zhang, M.-Y.; Wang, F.-D.; et al. A dual-function Cd-MOF with high proton conduction and excellent fluorescence detection of pyridine. *Dalton Trans.*. **2022**, *51*, 6687–6695. https://doi.org/10.1039/d2dt00193d.
22. Mai, Z.; Liu, D. Synthesis and Applications of Isoreticular Metal–Organic Frameworks IRMOFs-n (n = 1, 3, 6, 8). *Cryst. Growth Des.* **2019**, *19*, 7439–7462. https://doi.org/10.1021/acs.cgd.9b00879.
23. Nazir, M.A.; Khan, N.A.; Cheng, C.; et al. Surface induced growth of ZIF-67 at Co-layered double hydroxide: Removal of methylene blue and methyl orange from water. *Appl. Clay Sci.* **2020**, *190*, 105564. https://doi.org/10.1016/j.clay.2020.105564.

24. Bosch, M.; Yuan, S.; Rutledge, W.; et al. Stepwise Synthesis of Metal-Organic Frameworks. *Acc. Chem. Res.* **2017**, *50*, 857–865. https://doi.org/10.1021/acs.accounts.6b00457.
25. Niu, P.; Lu, N.; Liu, J.; et al. Water-induced synthesis of hierarchical Zr-based MOFs with enhanced adsorption capacity and catalytic activity. *Microporous Mesoporous Mater.* **2019**, *281*, 92–100. https://doi.org/10.1016/j.micromeso.2019.03.010.
26. Han, J.; Kong, D.; Zhou, W.; et al. Interface-engineering in MOF-derived In_2O_3 for highly sensitive and dual-functional gas sensor towards NO_2 and triethylamine. *Sens. Actuators B Chem.* **2023**, *395*, 134491. https://doi.org/10.1016/j.snb.2023.134491.
27. Rowsell, J.L.C.; Yaghi, O.M. Effects of Functionalization, Catenation, and Variation of the Metal Oxide and Organic Linking Units on the Low-Pressure Hydrogen Adsorption Properties of Metal−Organic Frameworks. *J. Am. Chem. Soc.* **2006**, *128*, 1304–1315. https://doi.org/10.1021/ja056639q.
28. Abdelhameed, R.M.; Carlos, L.D.; Silva, A.M.S.; et al. Engineering lanthanide-optical centres in IRMOF-3 by post-synthetic modification. *New J. Chem.* **2015**, *39*, 4249–4258. https://doi.org/10.1039/c4nj02382j.
29. Orefuwa, S.A.; Yang, H.; Goudy, A.J. Rapid solvothermal synthesis of an isoreticular metal–organic framework with permanent porosity for hydrogen storage. *Microporous Mesoporous Mater.* **2012**, *153*, 88–93. https://doi.org/10.1016/j.micromeso.2011.12.036.
30. Crom, A.B.; Strozier, J.L.; Tatebe, C.J.; et al. Deinterpenetration of IRMOF-9. *Chemistry* **2023**, *29*, e202302856. https://doi.org/10.1002/chem.202302856.
31. Rimi; Kumar, P.; Uttam, B.; et al. Highly Efficient Cauliflower-like Palladium-Loaded Porous MOF as a Robust Material for the Degradation of Organic Dyes. *ACS Omega* **2023**, *8*, 38895–38904. https://doi.org/10.1021/acsomega.3c03014.
32. Zheng, J.; Li, S.; Wang, Y.; et al. In situ growth of IRMOF-3 combined with ionic liquids to prepare solid-phase microextraction fibers. *Anal. Chim. Acta* **2014**, *829*, 22–27. https://doi.org/10.1016/j.aca.2014.04.039.
33. Venkata Sravani, V.; Tripathi, S.; Sreenivasulu, B.; et al. Post synthetically modified IRMOF-3 for efficient recovery and selective sensing of $U_{(vi)}$ from aqueous medium. *RSC Adv* **2021**, *11*, 28126–28137. https://doi.org/10.1039/d1ra02971a.
34. Sohrabnezhad, S.; Moghadamy, S. Zinc oxide nanorods incorporated magnetic isoreticular metal–organic framework for photodegradation of dyes. *J. Mol. Struct.* **2022**, *1247*, 131353. https://doi.org/10.1016/j.molstruc.2021.131353.
35. Isobe, T.; Arai, Y.; Yanagida, S.; et al. Solvothermal preparation and gas permeability of an IRMOF-3 membrane. *Microporous Mesoporous Mater.* **2017**, *241*, 218–225. https://doi.org/10.1016/j.micromeso.2016.12.031.
36. Ishak, M.A.I.; Jumbri, K.; Daud, S.; et al. Molecular simulation on the stability and adsorption properties of choline-based ionic liquids/IRMOF-1 hybrid composite for selective H_2S/CO_2 capture. *J. Hazard. Mater.* **2020**, *399*, 123008. https://doi.org/10.1016/j.jhazmat.2020.123008.
37. Liu, G.; Zhang, S.; Cai, Y.; et al. Morphology-tailored microwave absorption in MOF-derived Co_9S_8/Co@N, S dual-doped carbon composites via ligand-exchange induced progressive hollow engineering. *J. Alloys Compd.* **2024**, *983*, 173802. https://doi.org/10.1016/j.jallcom.2024.173802.
38. Zhang, Y.; Sun, Y.; Man, Y.; et al. Construction of a controllable and dispersed Fe_3O_4-based catalyst using ZIFs as a spatial support for highly catalytic degradation of aflatoxin B1. *Appl. Catal. B: Environ.* **2022**, *318*, 121818. https://doi.org/10.1016/j.apcatb.2022.121818.
39. Gao, F.; Tu, X.; Yu, Y.; et al. Core-shell Cu@C@ZIF-8 composite: A high-performance electrode material for electrochemical sensing of nitrite with high selectivity and sensitivity. *Nanotechnology* **2022**, *33*, 225501. https://doi.org/10.1088/1361-6528/ac3da7.
40. Qin, R.; Zeng, H.C. Design and Synthesis of Supported Nanoscale Metal–Organic Frameworks: Transformation from Transition Metal Silicates. *ACS Sustain. Chem. Eng.* **2018**, *6*, 14979–14988. https://doi.org/10.1021/acssuschemeng.8b03468.
41. Feng, Y.; Zhong, L.; Hou, Y.; et al. Acid-resistant enzyme@MOF nanocomposites with mesoporous silica shells for enzymatic applications in acidic environments. *J. Hazard. Mater.* **2019**, *306*, 54–61. https://doi.org/10.1016/j.jbiotec.2019.09.010.
42. Hosseini, S.R.; Omidkhah, M.; Mehri Lighvan, Z.; et al. Synthesis, characterization, and gas adsorption performance of an efficient hierarchical ZIF-11@ZIF-8 core–shell metal–organic framework (MOF). *Sep. Purif. Technol.* **2023**, *307*, 122679. https://doi.org/10.1016/j.seppur.2022.122679.
43. Xiang, L.; Liu, D.; Jin, H.; et al. Locking of phase transition in MOF ZIF-7: Improved selectivity in mixed-matrix membranes for O2/N2 separation. *Mater. Horiz.* **2020**, *7*, 223–228. https://doi.org/10.1039/c9mh00409b.
44. Koike, N.; Iyoki, K.; Wang, B.; et al. Increasing the ion-exchange capacity of MFI zeolites by introducing Zn to aluminosilicate frameworks. *Dalton Trans.* **2018**, *47*, 9546–9553. https://doi.org/10.1039/c8dt01391h.
45. Chang, J.; Wang, W.; Wang, Y.; et al. Fabrication of bimetallic Co/Zn leaf blade structure template derived Co_3O_4-ZIF/Zn and its ORR catalytic performance for MFC. *J. Taiwan Inst. Chem. Eng.* **2021**, *129*, 144–153. https://doi.org/10.1016/j.jtice.2021.09.027.
46. Wang, F.; Feng, T.; Jin, X.; et al. Atomic Co/Ni active sites assisted MOF-derived rich nitrogen-doped carbon hollow nanocages for enhanced lithium storage. *Chem. Eng. J.* **2021**, *420*, 127583. https://doi.org/10.1016/j.cej.2020.127583.

47. Gao, H.; Zhu, S.; Kang, Y.; et al. Zeolitic Imidazolate Framework-Derived Co-Fe@NC for Rechargeable Hybrid Sodium–Air Battery with a Low Voltage Gap and Long Cycle Life. *ACS Appl. Energy Mater.* **2022**, *5*, 1662–1671. https://doi.org/10.1021/acsaem.1c03073.
48. Saranya, V.; Athithya, S.; Sivalingam, M.M.; et al. Bifunctional carbon-wrapped CoCu electrocatalyst for superior water splitting and DSSC performance through work function optimization. *Int. J. Hydrogen Energy* **2024**, *91*, 380–392. https://doi.org/10.1016/j.ijhydene.2024.09.424.
49. Jiang, R.; Shu, P.; Yue, G.; et al. Construction of Co/Mn-ZIF@Ti_3C_2Tx composite via in-situ substitution on ZIF-67 for quasi-solid-state supercapacitor with high specific capacitance. *Chem. Eng. Sci.* **2025**, *302*, 120847. https://doi.org/10.1016/j.ces.2024.120847.
50. Jin, M.; Meng, S.; Liu, G.; et al. Construction of rose-type Co/Mo bimetal MOF and MOF-derived W embedded composites: Structure, reactivity, and dynamic simulation. *Mater. Res. Bull.* **2024**, *179*, 112927. https://doi.org/10.1016/j.materresbull.2024.112927.
51. Hao, J.; Jiang, Z.; Abbas Khan, H.; et al. Metal organic framework assisted Co-Ce mixed oxide catalyst for carbon monoxide and ethylene oxidation. *Fuel* **2022**, *318*, 123638. https://doi.org/10.1016/j.fuel.2022.123638.
52. Song, X.; Pan, Z.; Wang, Z.; et al. Metal–Organic Framework-Derived Porous Hollow Co_3O_4/ZnO Nanofibers for H_2S Sensing. *ACS Appl. Nano Mater.* **2024**, *7*, 8830–8841. https://doi.org/10.1021/acsanm.4c00300.
53. Rajpure, M.M.; Jadhav, H.S.; Kim, H. Advanced LDH-MOF derived bimetallic NiCoP electrocatalyst for methanol oxidation reaction. *Colloids Surf. A Physicochem. Eng. Asp.* **2022**, *654*, 130062 https://doi.org/10.1016/j.colsurfa.2022.130062.
54. Abraha, Y.W.; Tsai, C.-W.; Langner, E.H.G. De novo syntheses of multi-linker Zn- and Co-based ZIFs with application in CO2 fixation. *Microporous Mesoporous Mater.* **2022**, *346*, 112319 https://doi.org/10.1016/j.micromeso.2022.112319.
55. Wang, Y.; Zhao, X.; Yang, H.; et al. A Tale of Two Trimers from Two Different Worlds: A COF-Inspired Synthetic Strategy for Pore-Space Partitioning of MOFs. *Angew. Chem. Int. Ed.* **2019**, *58*, 6316–6320. https://doi.org/10.1002/anie.201901343.
56. Mei, S.; Chen, L.; Zhang, H.; et al. Assembling a Heterobimetallic Actinide Metal-Organic Framework by a Reaction-Induced Preorganization Strategy. *Angew. Chem. Int. Ed.* **2023**, *62*, e202306360. https://doi.org/10.1002/anie.202306360.
57. Luebke, R.; Belmabkhout, Y.; Weseliński, Ł.J.; et al. Versatile rare earth hexanuclear clusters for the design and synthesis of highly-connectedftw-MOFs. *Chem. Sci.* **2015**, *6*, 4095–4102. https://doi.org/10.1039/c5sc00614g.
58. Gao, W.-Y.; Pham, T.; Forrest, K.A.; et al. The local electric field favours more than exposed nitrogen atoms on CO_2 capture: A case study on the rht-type MOF platform. *Chem. Commun.* **2015**, *51*, 9636–9639. https://doi.org/10.1039/c5cc02573g.
59. Gong, X.; Noh, H.; Gianneschi, N.C.; et al. Interrogating Kinetic versus Thermodynamic Topologies of Metal-Organic Frameworks via Combined Transmission Electron Microscopy and X-ray Diffraction Analysis. *J. Am. Chem. Soc.* **2019**, *141*, 6146–6151. https://doi.org/10.1021/jacs.9b01789.
60. Xie, X.-J.; Zeng, H.; Xie, M.; et al. A metal-organic framework for C_2H_2/CO_2 separation under highly humid conditions: Balanced hydrophilicity/hydrophobicity. *Chem. Eng. J.* **2022**, *427*, 132033. https://doi.org/10.1016/j.cej.2021.132033.
61. Li, H.; Ren, X.; Pan, W.; et al. Enhanced peroxymonosulfate activation via MOF-derived bimetal core-shell Co-Fe@NC hybrids to degrade emerging pollutants. *J. Environ. Chem. Eng.* **2024**, *12*, 112062. https://doi.org/10.1016/j.jece.2024.112062.
62. Chen, S.; Qiu, Y.; Yu, S.; et al. Eu-MOF-based highly sensitive and selective luminescence probe for trace, in situ and visual detection of flunitrazepam. *Spectrochim. Acta Part A Mol. Biomol. Spectrosc.* **2025**, *326*, 125226. https://doi.org/10.1016/j.saa.2024.125226.
63. Li, S.; Chai, H.; Zhang, L.; et al. Constructing oxygen vacancy-rich MXene @Ce-MOF composites for enhanced energy storage and conversion. *J. Colloid Interface Sci.* **2023**, *642*, 235–245. https://doi.org/10.1016/j.jcis.2023.03.120.
64. Fu, Q.; Liu, D.; Niu, W.; et al. Defect-engineered MOF-808 with highly exposed Zr sites as highly efficient catalysts for catalytic transfer hydrogenation of furfural. *Fuel* **2022**, *327*, 125085. https://doi.org/10.1016/j.fuel.2022.125085.
65. Liu, Y.; Shen, D.; Tu, Z.; et al. Room-temperature hydrogen storage performance of metal-organic framework/graphene oxide composites by molecular simulations. *Int. J. Hydrogen Energy* **2022**, *47*, 41055–41068. https://doi.org/10.1016/j.ijhydene.2022.09.199.
66. Rezki, M.; Septiani, N.L.W.; Iqbal, M.; et al. Amine-functionalized Cu-MOF nanospheres towards label-free hepatitis B surface antigen electrochemical immunosensors. *J. Mater. Chem. B* **2021**, *9*, 5711–5721. https://doi.org/10.1039/d1tb00222h.
67. Bagheri, M.; Masoomi, M.Y. Quasi-metal organic frameworks: Preparation, applications and future perspectives. *Coord. Chem. Rev.* **2022**, *468*, 214643. https://doi.org/10.1016/j.ccr.2022.214643.
68. Su, H.; Pan, X.; Li, S.; et al. Defect-engineered two-dimensional transition metal dichalcogenides towards electrocatalytic hydrogen evolution reaction. *Carbon Energy* **2023**, *5*, e296. https://doi.org/10.1002/cey2.296.
69. Pei, Q.; Yuan, H.; Zhang, W.; et al. Engineering boundary-dominated topological states in defective hyperbolic lattices. *Phys. Rev. B* **2023**, *107*, 165145. https://doi.org/10.1103/PhysRevB.107.165145.
70. Wei, B.; Kong, N.; Hu, S.; et al. Effect of five typical vacancy defects on the tribological behaviors of MoS2 sheet: A molecular dynamics study. *Appl. Surf. Sci.* **2023**, *639*, 158175. https://doi.org/10.1016/j.apsusc.2023.158175.

71. Tao, Y.; Yang, B.; Wang, F.; et al. Green synthesis of MOF-808 with modulation of particle sizes and defects for efficient phosphate sequestration. *Sep. Purif. Technol.* **2022**, *300*, 121825. https://doi.org/10.1016/j.seppur.2022.121825.
72. Lim, J.; Lee, S.; Sharma, A.; et al. Ligand functionalization of defect-engineered Ni-MOF-74. *RSC Adv.* **2022**, *12*, 31451–31455. https://doi.org/10.1039/d2ra06587h.
73. Jin, L.; Zhou, C.; Chen, S.; et al. Controlled synthesis of defective MOF-808 and its application in levulinic acid esterification. *Appl. Catal. A: Gen.* **2024**, *681*, 119773. https://doi.org/10.1016/j.apcata.2024.119773.
74. Dashtipour, B.; Dehghanpour, S.; Sharbatdaran, M. Enhanced acidity of MOF-808 by defect-engineered and supported-sulfuric acid in ketalization of glycerol. *Polyhedron* **2024**, *247*, 116733. https://doi.org/10.1016/j.poly.2023.116733.
75. Huang, L.; Kong, X.; Chang, K.; et al. DBD plasma assisted synthesis of MO@Fe/Ce-MOFs with rich oxygen defects as efficient photocatalysts for nitrogen fixation. *J. Environ. Chem. Eng.* **2023**, *11*, 109836. https://doi.org/10.1016/j.jece.2023.109836.
76. Liu, H.; Fu, H.; Liu, Y.; et al. Synthesis, characterization and utilization of oxygen vacancy contained metal oxide semiconductors for energy and environmental catalysis. *Chemosphere* **2021**, *272*, 129534. https://doi.org/10.1016/j.chemosphere.2021.129534.
77. Zhao, Z.; Lei, R.; Zhang, Y.; et al. Defect controlled MOF-808 for seawater uranium capture with high capacity and selectivity. *J. Mol. Liq.* **2022**, *367*, 120514. https://doi.org/10.1016/j.molliq.2022.120514.
78. Zhang, Z.; Liu, C.; Chen, Y.; et al. Defect modulation of MIL-68(Fe) MOFs by Cu doping for boosting photocatalytic N2 fixation. *J. Catal.* **2024**, *432*, 115436. https://doi.org/10.1016/j.jcat.2024.115436.
79. Yu, L.; Zhang, Y.; Li, F.; et al. Efficient catalytic ozonation for hexazinone degradation by Fe/Ce-doped MOF derivatives. *Sep. Purif. Technol.* **2024**, *344*, 127277. https://doi.org/10.1016/j.seppur.2024.127277.
80. Rouhani, F.; Ghiasvand, M. Pore engineering of a Quasi-MOF-801 with unsaturated metal site and modulate porosity for selective and effective phosphate uptake. *Microporous Mesoporous Mater.* **2024**, *366*, 112941. https://doi.org/10.1016/j.micromeso.2023.112941.
81. Srivastava, P.; Marquez, G.P.; Gupta, S.; et al. Diversity of anaerobic ammonium oxidation processes in nature. *Chem. Eng. J.* **2024**, *483*, 149257. https://doi.org/10.1016/j.cej.2024.149257.
82. Nguyen, H.T.; Vo, V.O. Adsorption of VOCs onto Single Vacancy Defected Germanene Monolayer: A Study on Their Structure and Electronic Properties by DFT Calculations. *Pol. J. Environ. Stud.* **2023**, *32*, 3255–3265. https://doi.org/10.15244/pjoes/163346.
83. Han, J.; Chen, S.; Zhou, X.; et al. Uncovering growth species of multivariate MOFs in liquid phase by mass spectrometry. *Chin. Chem. Lett.* **2022**, *33*, 3993–3998. https://doi.org/10.1016/j.cclet.2021.11.035.
84. Liu, W.; Li, H.; Huang, D.; et al. Engineering α-MoO_3/TiO_2 heterostructures derived from MOFs/MXene hybrids for high-performance triethylamine sensor. *Chem. Eng. J.* **2024**, *483*, 149340. https://doi.org/10.1016/j.cej.2024.149340.
85. Urdapilleta-Inchaurregui, V.; Fernández-Luqueño, F.; Torres-Huerta, A.; et al. Natural Soil Clays from a Phaeozem to Synthesize a Nanocomposite with Exhausted Coffee Grounds and Ag- and TiO_2-Nanoparticles for Water, Air, or Soil Decontamination. *Pol. J. Environ. Stud.* **2020**, *30*, 871–880. https://doi.org/10.15244/pjoes/120521.
86. Rouhani, F.; Ayedi, M.; Safari, N. Dual nature brilliant adsorbent engineering by converting an Al-based MOF to defect rich quasi-MOF. *Sep. Purif. Technol.* **2024**, *331*, 125611. https://doi.org/10.1016/j.seppur.2023.125611.
87. Ngo, Q.; Nguyen, T.; Vo, M.; et al. Research on Synthesis of Composite Aerogels Based on PVA/Maltodextrine/Agar in Combination with Montmorillonite and Application in Tetracycline (TCC) Antibiotic Adsorption. *Pol. J. Environ. Stud.* **2023**, *33*, 313–320. https://doi.org/10.15244/pjoes/170776.
88. Gang, M.; Munir, A.; Murtaza, G.; et al. Agro-Waste-Based Bio-Nanocomposite for the Mitigation of Pb (II) Ions from Water. *Pol. J. Environ. Stud.* **2024**, *33*, 5635–5646. https://doi.org/10.15244/pjoes/183450.
89. Abánades Lázaro, I.; Forgan, R.S.; Cirujano, F.G. MOF nanoparticles as heterogeneous catalysts for direct amide bond formations. *Dalton Trans.* **2022**, *51*, 8368–8376. https://doi.org/10.1039/d2dt00369d.
90. Arul, P.; John, S.A. Size controlled synthesis of Ni-MOF using polyvinylpyrrolidone: New electrode material for the trace level determination of nitrobenzene. *J. Electroanal. Chem.* **2018**, *829*, 168–176. https://doi.org/10.1016/j.jelechem.2018.10.014.
91. Maxeiner, M.; Wittig, L.; Sedykh, A.E.; et al. Nano vs. bulk: Surfactant-controlled photophysical and morphological features of luminescent lanthanide MOFs. *J. Mater. Chem. A* **2023**, *11*, 22478–22491. https://doi.org/10.1039/d3ta05219b.
92. Rajagopal, N.; Uppara, H.P.; Dasari, H.; et al. Insights of MOF-derived bimetallic PVP/Ce-Ru nanocomposites for diesel soot oxidation. *Inorg. Chem. Commun.* **2023**, *155*, 111126. https://doi.org/10.1016/j.inoche.2023.111126.
93. Rashed, A.E.; Nasser, A.; Elkady, M.F.; et al. Fe Nanoparticle Size Control of the Fe-MOF-Derived Catalyst Using a Solvothermal Method: Effect on FTS Activity and Olefin Production. *ACS Omega* **2022**, *7*, 8403–8419. https://doi.org/10.1021/acsomega.1c05927.
94. Wang, S.; Lv, Y.; Yao, Y.; et al. Modulated synthesis of monodisperse MOF-5 crystals with tunable sizes and shapes. *Inorg. Chem. Commun.* **2018**, *93*, 56–60. https://doi.org/10.1016/j.inoche.2018.05.010.

95. Alazba, A.A.; Shafiq, M.; Amin, M.T. Transforming *Conocarpus* Hedge Waste into a Highly Effective Iron/Manganese Nanocomposite Biochar for Efficient Methylene Blue Dye Removal from Aqueous Solution. *Pol. J. Environ. Stud.* **2024**, *34*, 3033–3045. https://doi.org/10.15244/pjoes/188283.
96. Li, W.-Z.; Guo, F.-Y.; Li, J.; et al. Fabrication of bimetallic MOF-74 derived materials for high-efficiency adsorption of iodine. *Dalton Trans.* **2024**, *53*, 13370–13383. https://doi.org/10.1039/d4dt01554a.
97. Wei, L.; Li, M.; Zhang, Y.; et al. The role of Ca2+ in the improvement of phosphate adsorption in natural waters: Establishing an environmentally friendly La/Ca bimetallic organic framework. *Environ. Res.* **2023**, *219*, 115126. https://doi.org/10.1016/j.envres.2022.115126.
98. Shi, S.; Han, X.; Liu, J.; et al. Photothermal-boosted effect of binary Cu Fe bimetallic magnetic MOF heterojunction for high-performance photo-Fenton degradation of organic pollutants. *Sci. Total Environ.* **2021**, *795*, 148883. https://doi.org/10.1016/j.scitotenv.2021.148883.
99. Guo, J.; Ma, Y.; Li, P.; et al. Performance of a Kind of Novel Z-scheme Photocatalytic Catalysts: $CdMoO_4$/CNTs/g-C_3N_4. *Pol. J. Environ. Stud.* **2020**, *30*, 619–627. https://doi.org/10.15244/pjoes/123823.
100. Wang, R.; Han, J.; Yang, B.; et al. Defect Engineering in Metastable Phases of Transition-Metal Dichalcogenides for Electrochemical Applications. *Chem. Asian J.* **2020**, *15*, 3961–3972. https://doi.org/10.1002/asia.202000883.
101. López-Bermúdez, N.L.; Rodríguez-Torres, A.C.; Otálvaro-Álvarez, Á.M.; et al. Phosphate Adsorption from Aqueous Solutions Using Eggshell and Sacha Inchi (*Plukenetia volubilis*) Mixture. *Civ. Eng. J.* **2025**, *11*, 2918–2932. https://doi.org/10.28991/cej-2025-011-07-016.
102. Zhang, W.; Xu, Y.; Wang, Y.; et al. Double Z-Scheme Heterojunctions of CdS and ZnS Nanoparticles on Bimetallic Metal–Organic Frameworks for Photocatalytic H_2 Production. *ACS Appl. Nano Mater.* **2024**, *7*, 21993–22001. https://doi.org/10.1021/acsanm.4c04005.
103. Wang, Y.; Bai, X.; Huang, J.; et al. Tetrahydroxybenzoquinone-Based Two-Dimensional Conductive Metal–Organic Framework via π-d Conjugation Modulation for Enhanced Oxygen Evolution Reaction. *ACS Catal.* **2024**, *14*, 16532–16542. https://doi.org/10.1021/acscatal.4c04977.
104. Zhao, B.; Liu, J.; Liu, Y.; et al. In situ growth of ZnCdS nanoparticles on bimetallic Cu/Fe-MOF for efficient visible-light-driven photocatalytic hydrogen production and urea synthesis. *J. Alloys Compd.* **2025**, *1011*, 178395. https://doi.org/10.1016/j.jallcom.2024.178395.
105. Adekola, F.; Ayodele, S.; Inyinbor, A. Efficient Rhodamine B Removal Using Acidand Alkaline-Activated Musa paradisiaca Biochar. *Pol. J. Environ. Stud.* **2019**, *28*, 3063–3070. https://doi.org/10.15244/pjoes/94386.
106. Sarabia-Castillo, C.; Pérez-Moreno, A.; Fernández-Luqueño, F. Metal Oxide Nanoparticles (TiO_2, Zno, and Fe_2O_3) Change the Functional Groups, but not the Plant Tissue Content of Common Bean Plants Grown in a Greenhouse. *Pol. J. Environ. Stud.* **2023**, *32*, 1343–1352. https://doi.org/10.15244/pjoes/156777.
107. Wang, R.; Zhong, M.; Li, W.; et al. Isothermal and Kinetic Studies of Biosorption of Low Concentration Cr(III) from Aqueous Solution by 4 Microbial Biosorbents. *Pol. J. Environ. Stud.* **2022**, *31*, 1363–1376. https://doi.org/10.15244/pjoes/141903.
108. Xu, Z.; Ding, Y.; Huang, H.; et al. Biosorption Characteristics of Mn (II) by Bacillus cereus Strain HM-5 Isolated from Soil Contaminated by Manganese Ore. *Pol. J. Environ. Stud.* **2018**, *28*, 463–472. https://doi.org/10.15244/pjoes/84838.
109. Shi, R.; Zhang, Z.; Yang, F.; et al. Simultaneously anchoring free carboxyl and sulfonate groups into a metal-organic framework for high proton conductivity. *Microporous Mesoporous Mater.* **2022**, *343*, 112192. https://doi.org/10.1016/j.micromeso.2022.112192.
110. Meng, Y.; Wang, Y.; Liu, L.; et al. MOF modified with copolymers containing carboxyl and amidoxime groups and high efficiency U (VI) extraction from seawater. *Sep. Purif. Technol.* **2022**, *291*, 120946. https://doi.org/10.1016/j.seppur.2022.120946.
111. Bao, T.; Su, Y.; Zhang, N.; et al. Hydrophilic Carboxyl Cotton for in Situ Growth of UiO-66 and Its Application as Adsorbents. *Ind. Eng. Chem. Res.* **2019**, *58*, 20331–20339. https://doi.org/10.1021/acs.iecr.9b05172.
112. Liu, J.; Zhang, X.-Y.; Hou, J.-X.; et al. Functionalized Mn(II)-MOF based on host-guest interaction for selective and rapid capture of Congo red from water. *J. Solid State Chem.* **2019**, *270*, 697–704. https://doi.org/10.1016/j.jssc.2018.12.039.
113. Zhao, Y.; Wang, J.; Pei, R. Guest Molecules with Amino and Sulfhydryl Groups Enhance Photoluminescence by Reducing the Intermolecular Ligand-to-Metal Charge Transfer Process of Metal–Organic Frameworks. *Appl. Sci.* **2022**, *12*, 11467. https://doi.org/10.3390/app122211467.
114. Ji, J.; Liu, F.; Yang, W.; et al. Incorporation of Functional Groups in Porphyrinic Metal-Organic Frameworks by Post-modification for Highly Efficient Oxidation Catalysis. *ChemCatChem* **2020**, *12*, 4331–4338. https://doi.org/10.1002/cctc.202000295.
115. Song, S.; Ma, X.; Li, W.; et al. The influence of solvent controlled morphology on capacitive properties of metal-organic frameworks based on polyaminocarboxybenzene ligands. *Colloids Surf. A Physicochem. Eng. Asp.* **2023**, *656*, 130350. https://doi.org/10.1016/j.colsurfa.2022.130350.

116. Ji, G.; Han, Y.; Wang, J.; et al. A 3D Zn-MOF for luminescent sensing of p-nitrophenol and L-lysine, and enhanced proton conduction properties. *Dyes Pigm.* **2025**, *235*, 112601. https://doi.org/10.1016/j.dyepig.2024.112601.
117. Pan, W.; Wang, J.-P.; Sun, X.-B.; et al. Ultra uniform metal−organic framework-5 loading along electrospun chitosan/polyethylene oxide membrane fibers for efficient PM2.5 removal. *J. Clean. Prod.* **2021**, *291*, 125270. https://doi.org/10.1016/j.jclepro.2020.125270.
118. Zhao, X.; Gao, X.; Ding, R.; et al. Post-synthesis introduction of dual functional groups in metal–organic framework for enhanced adsorption of moxifloxacin antibiotic. *J. Colloid Interface Sci.* **2023**, *639*, 59–67. https://doi.org/10.1016/j.jcis.2023.02.035.
119. Ge, K.-M.; Wang, D.; Xu, Z.-J.; et al. A luminescent Eu(III)-MOF for selective sensing of Ag+ in aqueous solution. *J. Mol. Struct.* **2020**, *1208*, 127862. https://doi.org/10.1016/j.molstruc.2020.127862.
120. Hatakeyama, G.; Zhou, H.; Kikuchi, T.; et al. Design of a robust and strong-acid MOF platform for selective ammonium recovery and proton conductivity. *Chem. Sci.* **2023**, *14*, 9068–9073. https://doi.org/10.1039/d3sc02743k.
121. Talukder, N.; Wang, Y.; Tong, X.; et al. Chemical changes from N-doped graphene and Metal-Organic Frameworks to N-G/MOF composites for improved electrocatalytic activity. *Carbon* **2025**, *232*, 119816. https://doi.org/10.1016/j.carbon.2024.119816.
122. Liu, S.; Ma, X.; Liu, Y.; et al. Precisely modulating the branching functional groups of MIL-53(Al) for highly efficient sequestration of uranium. *J. Environ. Chem. Eng.* **2023**, *11*, 109393. https://doi.org/10.1016/j.jece.2023.109393.
123. Pan, H.; Xu, L.; Xu, T.; et al. Metal–Organic Frameworks for CO_2 Capture: Improving Adsorption Performance Through Modification Methods. *Nanomaterials* **2026**, *16*, 454. https://doi.org/10.3390/nano16080454.
124. Liu, B.; Liu, M.; Xie, Z.; et al. Performance of defective Zr-MOFs for the adsorption of anionic dyes. *J. Mater. Sci.* **2022**, *57*, 5438–5455. https://doi.org/10.1007/s10853-022-06874-w.
125. Rouhani, F.; Mousavifard, P. Tenfold increase in adsorption capacity of HKUST-1 toward Congo red by producing defective MOF under controlled thermal treatment. *Sep. Purif. Technol.* **2023**, *320*, 124230. https://doi.org/10.1016/j.seppur.2023.124230.
126. Fu, Y.; Yao, Y.; Forse, A.C.; et al. Solvent-derived defects suppress adsorption in MOF-74. *Nat. Commun.* **2023**, *14*, 2386. https://doi.org/10.1038/s41467-023-38155-8.
127. Xiang, Y.; Chen, X.; Zhang, L.; et al. Engineering Carbonic Anhydrase Mimics via Metal Ion Doping: Tailoring the Structure and Catalytic Properties of a 2-Aminoimidazole-Based MOF. *Langmuir* **2026**, *42*, 7398–7407. https://doi.org/10.1021/acs.langmuir.5c06793.
128. Shahzad, A.; Zulfiqar, F.; Arif Nadeem, M. Cobalt containing bimetallic ZIFs and their derivatives as OER electrocatalysts: A critical review. *Coord. Chem. Rev.* **2023**, *477*, 214925. https://doi.org/10.1016/j.ccr.2022.214925.
129. Lee, G.; Jhung, S.H. Obtaining both high CO2 adsorption capacity and CO_2/N_2 selectivity via blocking N_2 adsorption sites by grafting bulky diamine on metal–organic framework. *Fuel* **2025**, *394*, 135143. https://doi.org/10.1016/j.fuel.2025.135143.
130. Zhang, C.; Hu, B.; Ren, J.; et al. Thiol–Amino Bifunctional Metal–Organic-Framework-Based Membrane Regulating Hydrophobic Sites for Selective Separation of Artesunate. *Inorg. Chem.* **2024**, *63*, 14699–14711. https://doi.org/10.1021/acs.inorgchem.4c02295.
131. Shi, Z.-Q.; Ji, N.-N.; Du, J.; et al. Halogen-functionalized UiO-66-type metal–organic frameworks: From controlled syntheses and structure-property relationships to cross-disciplinary applications. *Coord. Chem. Rev.* **2026**, *566*, 218182. https://doi.org/10.1016/j.ccr.2026.218182.
132. Rodríguez-Sánchez, N.; Bhattacharya, B.; Emmerling, F.; et al. Engineering a multivariate cobalt metal–organic framework for high photocatalytic activity: The impact of mixed ligands and metal incorporation in a visible light-driven heterogeneous photo-Fenton reaction for water treatment. *Nanoscale Adv.* **2025**, *7*, 2255–2265. https://doi.org/10.1039/d4na00954a.
133. Jiang, Y.; Zhang, Z.; Du, Y.; et al. Tailoring the architecture of metal–organic frameworks: Precision etching for engineered defects and surfaces. *Green Energy Environ.* **2025**, *10*, 2107–2142. https://doi.org/10.1016/j.gee.2025.09.006.
134. Li, Y.-H.; Wang, C.-C.; Zeng, X.; et al. Seignette salt induced defects in Zr-MOFs for boosted Pb(II) adsorption: Universal strategy and mechanism insight. *Chem. Eng. J.* **2022**, *442*, 136276. https://doi.org/10.1016/j.cej.2022.136276.
135. He, Q.; Zhao, H.; Teng, Z.; et al. Tuning microscopic structure of La-MOFs via ligand engineering effect towards enhancing phosphate adsorption. *J. Environ. Manag.* **2024**, *353*, 120149. https://doi.org/10.1016/j.jenvman.2024.120149.
136. Gu, Y.; Luo, H.; Xu, W.; et al. Fabrication of MOF-808(Zr) with abundant defects by cleaving Zr O bond for oxidative desulfurization of fuel oil. *J. Ind. Eng. Chem.* **2022**, *105*, 435–445. https://doi.org/10.1016/j.jiec.2021.10.005.
137. Liu, Q.; Yang, J.-M.; Jin, L.-N.; et al. Metal ion induced porous HKUST-1 nano/microcrystals with controllable morphology and size. *CrystEngComm* **2016**, *18*, 4127–4132. https://doi.org/10.1039/c5ce02497h.
138. You, D.; Shi, H.; Yang, L.; et al. Tuning the Sb(V) adsorption performance of La-MOFs via ligand engineering effect: Combined experiments with theoretical calculations. *Chem. Eng. J.* **2022**, *435*, 134874. https://doi.org/10.1016/j.cej.2022.134874.

139. Qian, S.; Kamaruddin, M.A.B.; Kai, H.; et al. Study on Preparation of Nano Humic Acid and Adsorption Effect of Heavy Metals in Soil. *Emerg. Sci. J.* **2025**, *9*, 2350–2366. https://doi.org/10.28991/esj-2025-09-05-04.
140. Rae, I.B.; Gibb, S.W. Removal of metals from aqueous solutions using natural chitinous materials. *Water Sci. Technol.* **2003**, *47*, 189–196. https://doi.org/10.2166/wst.2003.0572.
141. Tang, J.; Xiang, L. Development of a Probe Based on Quantum Dots Embedded with Molecularly Imprinted Polymers to Detect Parathion. *Pol. J. Environ. Stud.* **2016**, *25*, 787–793. https://doi.org/10.15244/pjoes/60888.
142. Hussain Shah, J.; Sharif, S.; Şahin, O.; et al. A dual-emitting Rhodamine B-encapsulated Zn-based MOF for the selective sensing of Chromium(VI). *Spectrochim. Acta Part A Mol. Biomol. Spectrosc.* **2024**, *310*, 123899. https://doi.org/10.1016/j.saa.2024.123899.
143. Xu, O.; Wan, S.; Yang, J.; et al. Ni-MOF Functionalized Carbon Dots with Fluorescence and Adsorption Performance for Rapid Detection of Fe (III) and Ascorbic Acid. *J. Fluoresc.* **2022**, *32*, 1743–1754. https://doi.org/10.1007/s10895-022-02982-7.
144. Meng, H.; Zhao, C.; Li, Y.; et al. An implanted paramagnetic metallofullerene probe within a metal–organic framework. *Nanoscale* **2018**, *10*, 3291–3298. https://doi.org/10.1039/c7nr09420e.
145. Du, Q.; Wu, P.; Dramou, P.; et al. One-step fabrication of a boric acid-functionalized lanthanide metal–organic framework as a ratiometric fluorescence sensor for the selective recognition of dopamine. *New J. Chem.* **2019**, *43*, 1291–1298. https://doi.org/10.1039/c8nj05318a.
146. Vellingiri, K.; Deep, A.; Kim, K.-H.; et al. The sensitive detection of formaldehyde in aqueous media using zirconium-based metal organic frameworks. *Sens. Actuators B Chem.* **2017**, *241*, 938–948. https://doi.org/10.1016/j.snb.2016.11.017.
147. Eskandari, H.; Amirzehni, M.; Hassanzadeh, J.; et al. Mesoporous MIP-capped luminescent MOF as specific and sensitive analytical probe: Application for chlorpyrifos. *Mikrochim Acta* **2020**, *187*, 673. https://doi.org/10.1007/s00604-020-04654-4.
148. Guo, J.; Wan, Y.; Zhu, Y.; et al. Advanced photocatalysts based on metal nanoparticle/metal-organic framework composites. *Nano Res.* **2020**, *14*, 2037–2052. https://doi.org/10.1007/s12274-020-3182-1.
149. Zhao, L.; Xu, G.; Gao, C.; et al. A novel RhB@MOF-808 fluorescent probe for the rapid detection of dopamine and Fe^{3+} *Anal. Biochem.* **2023**, *671*, 115154. https://doi.org/10.1016/j.ab.2023.115154.
150. Dharman, R.K.; Mariappan, A.; Oh, T.H. Accelerated photocatalytic degradation of sulfonamide antibiotic pollutant using oxygen vacancy in metal-organic framework ZIF-8/Ag3PO4 heterostructure. *Surf. Interfaces* **2023**, *39*, 102998. https://doi.org/10.1016/j.surfin.2023.102998.
151. Meng, J.; He, M.; Li, F.; et al. Combining Ce-metal–organic framework with CdS for efficient photocatalytic removals of heavy metal ion and organic pollutant under visible and solar lights. *Inorganica Chim. Acta* **2023**, *557*, 121701. https://doi.org/10.1016/j.ica.2023.121701.
152. Sadeghi, S.; Najafidoust, A.; Haeri, S.Z.; et al. Defective MIL-88B(Fe) metal-organic frameworks: Peculiar photocatalysts for enhanced degradation of organic pollutants. *Inorg. Chem. Commun.* **2025**, *180*, 114956. https://doi.org/10.1016/j.inoche.2025.114956.
153. Liu, S.; Yang, Y.; Xiao, W.; et al. Metal-organic frameworks derived porous MoS_2/CdS heterostructure for efficient photocatalytic performance towards hydrogen evolution and organic pollutants. *Int. J. Hydrogen Energy* **2023**, *48*, 32729–32738. https://doi.org/10.1016/j.ijhydene.2023.05.050.
154. Dong, R.; Wang, F.; Zhao, S.; et al. Photocatalytic degradation of organic pollutants by porphyrin metal-organic framework: Structural engineering, design strategies, and environmental applications. *Rev. Mater. Res.* **2025**, *1*, 100066. https://doi.org/10.1016/j.revmat.2025.100066.
155. El-Sayyad, G.S.; El-Khawaga, A.M.; Rashdan, H.R.M. Gamma-irradiated copper-based metal organic framework nanocomposites for photocatalytic degradation of water pollutants and disinfection of some pathogenic bacteria and fungi. *BMC Microbiol.* **2024**, *24*, 453. https://doi.org/10.1186/s12866-024-03587-9.
156. Abdurahman, M.H.; Rhimi, B.; El-Khodary, S.A.; et al. Structural tailoring of metal–organic frameworks for photocatalytic degradation of contaminant emergence concern: Recent advances and perspectives. *Sep. Purif. Technol.* **2025**, *376*, 134016. https://doi.org/10.1016/j.seppur.2025.134016.
157. Bai, Z.; Zhao, X.; Yu, S.; et al. The one-pot synthesis of defect-rich bimetallic MOFs for efficient photocatalytic Fenton degradation of organic pollutants. *J. Alloys Compd.* **2024**, *1008*, 176589. https://doi.org/10.1016/j.jallcom.2024.176589.
158. Yu, S.; Tang, H.; Zhang, D.; et al. MXenes as emerging nanomaterials in water purification and environmental remediation. *Sci. Total Environ.* **2022**, *811*, 152280. https://doi.org/10.1016/j.scitotenv.2021.152280.
159. Chen, H.; Wang, J. MOF-derived Co3O4-C@FeOOH as an efficient catalyst for catalytic ozonation of norfloxacin. *J. Hazard. Mater.* **2021**, *403*, 123697. https://doi.org/10.1016/j.jhazmat.2020.123697.
160. Meng, H.; Chang, J.; Wang, S.; et al. Fabrication of MOF-carbonized materials as ozone catalysts for water purification: Exploration of catalytic mechanisms. *J. Environ. Chem. Eng.* **2024**, *12*, 114632. https://doi.org/10.1016/j.jece.2024.114632.

161. Usman, M.; Cheema, S.A.; Farooq, M. Heterogeneous Fenton and persulfate oxidation for treatment of landfill leachate: A review supplement. *J. Clean. Prod.* **2020**, *256*, 120448. https://doi.org/10.1016/j.jclepro.2020.120448.
162. Wang, J.; Wang, S. Activation of persulfate (PS) and peroxymonosulfate (PMS) and application for the degradation of emerging contaminants. *Chem. Eng. J.* **2018**, *334*, 1502–1517. https://doi.org/10.1016/j.cej.2017.11.059.
163. Fan, Y.-H.; Li, Y.-Q.; Hayat, F.; et al. Multi-targeted removal of coexisted antibiotics in water by the synergies of radical and non-radical pathways in PMS activation. *Sep. Purif. Technol.* **2023**, *305*, 122475. https://doi.org/10.1016/j.seppur.2022.122475.
164. Yao, J.; Chen, Z.; Zhang, H.; et al. New insight into the regulation mechanism of visible light in naproxen degradation via activation of peroxymonosulfate by MOF derived $BiFeO_3$. *J. Hazard. Mater.* **2022**, *431*, 128513. https://doi.org/10.1016/j.jhazmat.2022.128513.
165. Kumar, P.; Anand, B.; Tsang, Y.F.; et al. Regeneration, degradation, and toxicity effect of MOFs: Opportunities and challenges. *Environ. Res.* **2019**, *176*, 108488. https://doi.org/10.1016/j.envres.2019.05.019.
166. Cai, J.; Zhang, J.; Shi, J.; et al. Defective UiO-66-NH_2 (Zr) for Simultaneous Adsorption of Phosphate and Pb^{2+} for Hydrogen Peroxide Purification. *Inorg. Chem.* **2024**, *63*, 7314–7324. https://doi.org/10.1021/acs.inorgchem.4c00179.
167. Forghani, M.; Azizi, A.; Livani, M.J.; et al. Adsorption of lead(II) and chromium(VI) from aqueous environment onto metal-organic framework MIL-100(Fe): Synthesis, kinetics, equilibrium and thermodynamics. *J. Solid State Chem.* **2020**, *291*, 121636. https://doi.org/10.1016/j.jssc.2020.121636.
168. Sharma, R.; Padunnappattu, A.; Van der Stricht, M.P.; et al. Structured Aluminum Phosphonate Metal–Organic Framework for Efficient Hydrogen Purification: Reversible HCl Adsorption and Water-Triggered Regeneration. *Chem. Mater.* **2026**, *38*, 7083–7094. https://doi.org/10.1021/acs.chemmater.5c03397.
169. Lirio, S.; Kao, S.-H.; Lai, Y.-L.; et al. Functional group directed tuning of highly recyclable Zr-MOF beads for preferential VOC adsorption. *Microporous Mesoporous Mater.* **2025**, *395*, 113700. https://doi.org/10.1016/j.micromeso.2025.113700.
170. Felder, T.M.O.; Taheri, N.; Schertenleib, T.; et al. Efficient, Reversible Lead Adsorption in a Thiol-Decorated Zirconium-Metal–Organic Framework. *Small* **2026**, *22*, e13162. https://doi.org/10.1002/smll.202513162.
171. Thi Thanh, M.; Vinh Thien, T.; Thi Thanh Chau, V.; et al. Synthesis of Iron Doped Zeolite Imidazolate Framework-8 and Its Remazol Deep Black RGB Dye Adsorption Ability. *J. Chem.* **2017**, *2017*, 5045973. https://doi.org/10.1155/2017/5045973.
172. Sadiq, M.M.; Batten, M.P.; Mulet, X.; et al. A Pilot-Scale Demonstration of Mobile Direct Air Capture Using Metal-Organic Frameworks. *Adv. Sustain. Syst.* **2020**, *4*, 2000101. https://doi.org/10.1002/adsu.202000101.
173. Liu, H.; Li, N.; Feng, M.; et al. Near-infrared light induced adsorption–desorption cycle for VOC recovery by integration of metal–organic frameworks with graphene oxide nanosheets. *Environ. Sci. Nano* **2022**, *9*, 1858–1868. https://doi.org/10.1039/d2en00103a.
174. Liu, X.; Cheng, X.; Lian, J.; et al. Z-scheme heterojunction BiOBr/MIL-100(Fe) visible photocatalytic-permonosulfate degradation of AO7. *Water Sci. Technol.* **2025**, *91*, 363–381. https://doi.org/10.2166/wst.2025.010.
175. Jiang, S.; Xu, L.; Wu, F.; et al. Structurally stable Ag/Ag2O@MOF-808 photocatalysts for efficient photodegradation of high-concentration Rhodamine B. *J. Photochem. Photobiol. A Chem.* **2026**, *472*, 116789. https://doi.org/10.1016/j.jphotochem.2025.116789.